NeuroImage: Clinical 36 (2022) 103190

Contents lists available at ScienceDirect

NeuroImage: Clinical

journal homepage: www.elsevier.com/locate/ynicl

The longitudinal neural dynamics changes of whole brain connectome during natural recovery from poststroke aphasia

Liming Fan [a,b], Chenxi Li [d], Zi-gang Huang [a,b], Jie Zhao [a,b], Xiaofeng Wu [a,b], Tian Liu [a,b], Youjun Li [a,b,*], Jue Wang [a,b,c,*]

[a] The Key Laboratory of Biomedical Information Engineering of Ministry of Education, Institute of Health and Rehabilitation Science, School of Life Science and Technology, Xi'an Jiaotong University, Xi'an, Shaanxi 710049, PR China
[b] National Engineering Research Center of Health Care and Medical Devices. Guangzhou, Guangdong 510500, PR China
[c] The Key Laboratory of Neuro-informatics & Rehabilitation Engineering of Ministry of Civil Affairs, Xi'an, Shaanxi 710049, PR China
[d] Department of the Psychology of Military Medicine, Air Force Medical University, Xi'an, Shaanxi 710032, PR China

ARTICLE INFO

Keywords:
Post-stroke aphasia
fMRI
Energy landscape
Major states
Brain flexibility

ABSTRACT

Poststroke aphasia is one of the most dramatic functional deficits that results from direct damage of focal brain regions and dysfunction of large-scale brain networks. The reconstruction of language function depends on the hierarchical whole-brain dynamic reorganization. However, investigations into the longitudinal neural changes of large-scale brain networks for poststroke aphasia remain scarce. Here we characterize large-scale brain dynamics in left-frontal-stroke aphasia through energy landscape analysis. Using fMRI during an auditory comprehension task, we find that aphasia patients suffer serious whole-brain dynamics perturbation in the acute and subacute stages after stroke, in which the brains were restricted into two major activity patterns. Following spontaneous recovery process, the brain flexibility improved in the chronic stage. Critically, we demonstrated that the abnormal neural dynamics are correlated with the aberrant brain network coordination. Taken together, the energy landscape analysis exhibited that the acute poststroke aphasia has a constrained, low dimensional brain dynamics, which were replaced by less constrained and high dimensional dynamics at chronic aphasia. Our study provides a new perspective to profoundly understand the pathological mechanisms of poststroke aphasia.

1. Introduction

Aphasia is one of the most severe and prevalent functional impairments following stroke that negatively impacts the daily quality of life of patients (Flowers et al., 2016; Gerstenecker and Lazar, 2019; Kiran and Thompson, 2019). To develop novel, targeted and efficient treatment strategies, it is essential to understand the neural mechanisms underlying spontaneous language function rehabilitation.

Language function has always been ascribed to the effects of separated motor or sensory language cores, such as Broca's area and Wernicke's area, and the direct fiber connections or functional circuitry between them. These theoretical frameworks have predominated for several decades (Dick et al., 2014; Tremblay and Dick, 2016; Nasios et al., 2019). Modern views suggest that the brain is organized into a set of anatomically distributed but functionally integrated large-scale networks (Cole et al., 2014; Xu et al., 2021). The classic theories seem outdated because they do not comprehensively consider language-related distributed functional connectivity and are constrained from the perspectives of modular or central language areas; otherwise, little is known about subcortical structures and the cerebellum. Modern neuroimaging and neural computational studies give us a deeper and more comprehensive understanding of language function and shed new light on language recovery after poststroke aphasia. In summary, these multimodal and multiscale studies emphasize that successful language processing should rely on interactions of the multiple brain functional systems. This complex, high-order cognitive system comprises the cerebral cortex (Vigneau et al., 2006; Vigneau et al., 2011; Vasa et al., 2015; Hartwigsen and Saur, 2019; Stockert et al., 2020; Ding et al., 2020; Xu et al., 2020; Branco, Seixas, and Castro, 2020), subcortex (Crosson, 1985; Chenery, Copland, and Murdoch, 2002; Copland, 2003; Herbet et al., 2016; Broser et al., 2012; Cignetti et al., 2020) and cerebellum (Murdoch, 2010; Ackermann, 2013; Schwartze and Kotz, 2016;

* Corresponding authors at: The Key Laboratory of Biomedical Information Engineering of Ministry of Education, and Institute of Biomedical Engineering, School of Life Science and Technology, Xi'an Jiaotong University, Xi'an 710049, PR China.
E-mail addresses: liyoujun1@mail.xjtu.edu.cn (Y. Li), juewang_xjtu@126.com (J. Wang).

https://doi.org/10.1016/j.nicl.2022.103190
Received 25 February 2022; Received in revised form 24 July 2022; Accepted 8 September 2022
Available online 13 September 2022
2213-1582/© 2022 The Author(s). Published by Elsevier Inc. This is an open access article under the CC BY-NC-ND license (http://creativecommons.org/licenses/by-nc-nd/4.0/).

Moberget et al., 2016; Mariën and Borgatti, 2018; Ashida et al., 2019; Geva et al., 2021). This system is conceptually described as a language connectome, which works via cortico-cortical communication, cortico-subcortical communication and cerebello-cortical interactions (Fedorenko and Thompson-Schill, 2014; Dick et al., 2014). Given the above perspective, poststroke aphasia can be considered a network disorder related to multiple large-scale networks (Carter et al., 2012; Thiel and Zumbansen, 2016; Siegel et al., 2016; Stockert and Saur, 2017; Stockert et al., 2020).

Previous neuroimage studies in post-stroke aphasia have proposed that successful language reorganization should rely on 1) language-specific networks, which are mainly left-lateralized frontotemporal networks (Winhuisen et al., 2007; Thiel et al., 2013; Griffis et al., 2017; Fridriksson et al., 2012; Fridriksson et al., 2010; Ding et al., 2020), 2) recruitment of lesion-homologue areas in right hemisphere (Winhuisen et al., 2007, 2005; Xing et al., 2016; Turkeltaub et al., 2012; Meltzer et al., 2013; Kourtidou et al., 2021; Harvey et al., 2017; François et al., 2019), 3) bilateral domain-general multidemand systems (Geranmayeh et al., 2014; Geranmayeh et al., 2017; Saur et al., 2006; Stockert et al., 2020; Stockert and Saur, 2017) involving a frontoparietal network and a cingulo-opercular network under situation of large lesions or incomplete recovery. Disrupted functional connectivity (FC) within and across these large-scale functional networks account for language deficits for post-stroke aphasia (Siegel et al., 2018; Siegel et al., 2016; Duncan and Small, 2018; Carter et al., 2012). In most of the FC studies, a common assumption is spatially and temporally static brain during the scan, which is an average quantity of the brain activity. The study of temporal variability of the brain activity and connectivity is an emerging area, which can capture the spontaneous and reoccurring activity patterns of functional brain networks during resting period, performing tasks or suffering perturbations (Freyer et al., 2011; Deco and Jirsa, 2012; Deco et al., 2013; Wang et al., 2013; Tognoli and Kelso, 2014; Hansen et al., 2015; Chen and Huang, 2017; Sayal et al., 2020). By using a dynamic framework, (Guo et al., 2019) has reported that dynamic segregation and integration of spatiotemporal information across large-scale brain networks may account for language disruptions in post-stroke aphasia. Nonetheless, what changes occur to the neural dynamics of the whole brain when dramatic local damage occurs and how the neural activity patterns of large-scale networks transit dynamically to mitigate attacks are still poorly explored with respect to the natural recovery of post-stroke aphasia patients from the acute stage to the chronic stage. We hypothesize that the brains of poststroke aphasia patients and healthy individuals exhibit various neural activity traversals patterns among canonical brain states, and the characteristics of these traversals are different among acute, subacute and chronic brain stage.

To test these hypotheses, energy landscape analysis, which is rooted in statistical physics and applied to study the fluctuations of blood oxygenation level-dependent (BOLD) fMRI of large-scale human brain networks (Watanabe et al., 2013; Watanabe and Rees, 2017; Riehl et al., 2018; Kang et al., 2017; Kang et al., 2021), was applied in our research. Energy landscape analysis had already been applied to describe the dynamics of high-dimensional biological systems (Kapon, Nevo, and Reich, 2008; Wolynes, 2015; Neelamraju, Gosavi, and Wales, 2018; Zhang and Wolynes, 2017; Ross-Naylor, Mijajlovic, and Biggs, 2020; Stewman, Tsui, and Ma, 2020) and other systems (Othayoth, Thoms, and Li, 2020) to explore the intrinsic complicacies. Recently, it was introduced to the field of brain research to study the brain dynamics (Watanabe et al., 2013; Watanabe et al., 2014; Ashourvan et al., 2017; Kang et al., 2017; Watanabe and Rees, 2017; Gu et al., 2018; Kang et al., 2021). In the energy landscape analysis, brain states were defined as the activity patterns across brain regions or large-scale functional networks (Watanabe et al., 2013; Watanabe et al., 2014; Ashourvan et al., 2017; Kang et al., 2017; Watanabe and Rees, 2017; Gu et al., 2018; Kang et al., 2021). On the basis of the Boltzmann distribution of the states, the energy of a state was calculated by the negative log appearance probability of the state. However, it should be noted that the energy we introduced here actually represented the appearance frequency of state rather than biologically significant terminology. Thus, a state that possessed a larger probability of occurrence had a lower energy. The hierarchical relationship (inverse frequency distribution) among the energy values of all possible brain activity patterns across the regions of interest (ROIs) was used to define an energy landscape (Fig. 1a-le).

In the present study, we constructed energy landscapes using a pairwise maximum entropy model (MEM) (equivalent to the Ising model and the Boltzmann machine) of BOLD-fMRI data collected from 16 left frontal post-stroke aphasia patients in the acute (1–7 days), subacute (1–3 weeks), and chronic stages (more than half a year) and 17 age-matched healthy subjects when they performed an auditory short sentence comprehension task published in recent research (Stockert et al., 2020). This is because the energy landscape can dramatically simplify the problem of characterizing the multistability of neural networks, automatically identifying relatively frequent and dominant brain activity patterns in high-dimensional neural data without any priori information, and delineating neural dynamics as staying in and moving between these brain states (Watanabe et al., 2013; Watanabe et al., 2014; Ashourvan et al., 2017; Kang et al., 2017; Watanabe and Rees, 2017; Gu et al., 2018; Kang et al., 2021). Previous approaches help us to comprehend the detailed workings of a specific language system in aphasia and their temporal correlation, but the information about higher-order interactions (Watanabe et al., 2013) was disregarded, the energy landscape was supposed to complement our knowledge of how brain activity rapidly reconfigures the large-scale functional systems architecture to facilitate communication between segregated cortical regions and cerebellum/subcortical structures during cognitive tasks. Otherwise, energy landscape analysis can identify what might be obscured states in the multistable brain and resolve the challenging tasks of system-level interpretation relatively intuitionistic (Munn et al., 2021). Technically, for each of the four groups (healthy control (T0) and left frontal post-stroke aphasia at acute stage (T1), subacute stage (T2) and chronic stage (T3)), we first estimated an energy landscape and then mapped brain dynamics to the movement of a 'ball' on this energy landscape. States with the lower positions in the dendriform graph (dysconnectivity graph) had smaller energy values and appeared more frequently. On the basis of these energy values, we extracted local minima and transition paths among them from the energy landscape and compared the brain dynamics indices among the four groups. We further investigated the relationships between these indices and language evaluation scores (language production (LRS_{PROD}) and language comprehension (LRS_{COMP}) scores). Finally, we explored the neural basis underlining these brain dynamics by investigating the relationships between brain segregation strength levels based on the major states and dynamics of the brain.

2. Materials and methods

2.1. Subjects

All neuroimage and behavioral data we used here have been reported in a previous publication (Stockert et al., 2020) and were available through the figshare repository (https://doi.org/10.6084/m9.figshare.7093481). The 16 patients (one subject (ID: 09) was discarded because of the incompletely shared fMRI data) with first ischemic stroke of the left frontal cortex and 17 age-matched normal individuals were involved in our analyses. The spatial similarity of lesion patterns was confirmed in (Stockert et al., 2020). All patients were enrolled, scanned and behaviorally evaluated longitudinally at the acute stage (T1 = 1–7 days after stroke), subacute stage, (T2 = 8–21 days after stroke) and chronic stage after stroke (T3, > half a year). The normal subjects were scanned only once. The approval of local Ethics Committee has been reported in (Saur et al., 2006).

Behavioral assessments were performed using a clinically standard Aachen Aphasia Test (AAT) diagnostic battery for language modalities

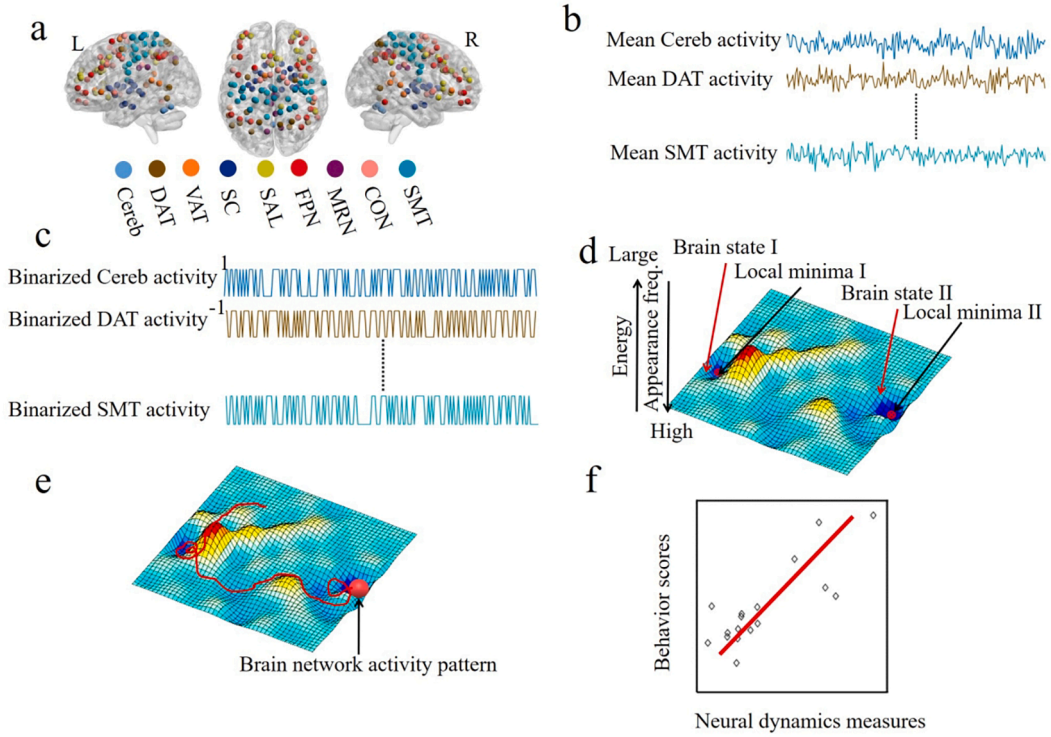

Fig. 1. Pipeline of energy landscape analysis. (a-f) We extracted fMRI signals from 131 ROIs (a), and then assigned these ROIs into nine large-scale functionally nonoverlapping brain networks and calculated the average network activity (b). For each ROI, we then binarized the continuous time series based on the mean of the average network activity (c). We fitted a pairwise maximum entropy model to build an energy landscape applied to the binarized fMRI series, and identified dominant brain states (d). After that, we characterized the whole brain neural dynamics using a MCMC numerical simulation processing (e). Finally, we investigated the relationships between several brain dynamic indices and behavioral assessment scores (f). It should be noted that the energy values that we mentioned here only indicate the appearance probability of all the possible 2^9 brain states. SMT: Somatosensory and motor network; CON: Cingulo-opercular network; MRN: Memory retrieval network; FPN: Frontoparietal network; SAL: Salience network; SC: Subcortical; VAT: Ventral attention network; DAT: Dorsal attention network; Cereb: Cerebellum. L: left; R: right.

and phenotype classification of poststroke aphasia for the acute, subacute and chronic phases. According to the subtest scores, the AAT scores were normalized and averaged into a synthetic evaluation, which included language comprehension (LRS_{COMP}) and production (LRS_{PROD}) scores (range: 0–1; 1 indicated the superior performance).

2.2. Image acquisition

Functional and structural MRIs were collected with a 3.0 T Siemens TRIO TIM or VERIO MR scanner with standard protocols during an auditory comprehension task. High-resolution T1-weighted anatomical data were acquired using an MP-RAGE sequence (TR = 2.2 s, TE = 2.6 ms, FOV = 160 × 240 mm, 160 slices, voxel size 1 × 1 × 1 mm) for the lesion mapping, spatial preprocessing and spatial normalization of the fMRI data. Functional MRI data were obtained by applying a gradient echoplanar imaging (*EPI*) sequence (TR = 1.83 or 2.19 s, TE = 25 or 96 ms, 115 or 260 scans, 32 or 36 axial slices, flip angle = 70 or 75°, FOV = 192 × 192 mm, voxel size 3 × 3 × 3 mm, slice gap = 1 mm, matrix = 64 × 64 for paradigms I and II, respectively). Diffusion-weighted data were acquired using an *EPI* sequence (TR = 4.8 s, TE = 105.2 ms, slice thickness = 6 mm, matrix = 256 × 256, FOV = 240 × 240 mm).

2.3. Lesion mapping and fMRI preprocessing

A detailed description of lesion mapping and fMRI preprocessing has been previously reported in (Stockert et al., 2020). Here we summarized the important steps. For lesion mapping, a trained neurologist drew the lesions on diffusion-weighted images (DWI) using MRIcron. The following steps were performed with SPM12. First, the functional images were corrected for slice acquisition time and head movement within and between scanning sessions. Second, the high-resolution T1-weighted scan was co-registered to the mean of the realigned functional scan. Third, the DWI images and binary lesion masks were co-registered to match the respective T1-weighted image, which was then normalized to standard Montreal Neurological Institute (MNI) space. Fourth, the realigned functional images were then normalized with the resulting matrices in step three and smoothed with a 4 mm full-width half maximum (FWHM) Gaussian kernel.

For the following analysis, we additionally removed the nuisance signal through linear regression: 24 head motion regressors estimated based on the Friston-24 Parameters, global signal, white matter and cerebrospinal fluid (CSF) signals with the MATLAB toolbox, DPARSF (Chao-Gan and Yu-Feng, 2010).

2.4. Rois selection and functional networks arrangement.

We then extracted the time series of BOLD signals for each session and group from each of the 131 ROIs (Supplementary Table 1). The 131 ROIs were defined as 5-mm spheres around the center coordinates. Initially, we selected 9 wide reported functional brain networks that included 134 ROIs in Power's brain map (Power et al., 2011); (b) we checked the location for every 134 ROIs MNI central coordinates with MRIcron in normalized functional MRI for every aphasia patient; (c) We only excluded the ROIs that fell in the lesion totally because of the limit spatial resolution of the functional scan. in this step, 5 ROIs were excluded (Supplementary Table 2); (d) We then excluded 4 ROIs that had poor overlap with the brain of the patient group (Supplementary Table 2), after this, 125 ROIs were selected. (e) We selected 6 wide

reported sub-cortical structures by literature review (bilateral amygdala and caudate in basal ganglia, bilateral hippocampus), because of their important function in semantic memory (Duff et al., 2019; Klooster et al., 2020) and language processing (Shaw et al., 2016; Shi and Zhang, 2020). These 6 ROIs were also defined as 5-mm spheres around the center coordinates based on AAL atlas (Tzourio-Mazoyer et al., 2002). (f) Finally, we arranged the 131 ROIs into 9 functional networks (Supplementary Fig. 1) (somatosensory and motor network (SMT), cingulo-opercular network (CON), memory retrieval network (MRN), fronto-parietal network (FPN), salience network (SAL), subcortical system (SC), ventral attention network (VAT), dorsal attention network (DAT) and cerebellum system (Cereb)) based on the Power's functional brain systems (Power et al., 2011) (Fig. 1a). We visualized the results of functional network arrangement using BrainNet Viewer (Xia et al., 2013). Finally, we calculated the average network activity per session.

2.5. Fitting a pairwise MEM

As in previous studies, a pairwise MEM was estimated for the binarized fMRI data extracted from the 9 networks for each group respectively (Gu et al., 2018; Watanabe and Rees, 2017). The pairwise MEM and the model fitting procedures are briefly described as follows.

For each participant, we calculated the average value of the signals obtained during each session. For the following model fitting and energy landscape analysis process, normalized continuous fMRI signals were binarized according to the average value of each session (+1 indicates the fMRI signal was greater than average activity, otherwise, the value equals −1) (Ezaki et al., 2017) and concatenated across participants. Though the aforementioned preprocessing approach, nine concatenated binary time series data representing nine network activities were finally obtained for healthy controls and each stage of the patient groups.

Then a pairwise MEM was fitted to the nine binary time series data with the same method as that used in previous studies for each group. First, the binarized activity of network i at a discrete time t was denoted by σ_i^t ($\sigma_i^t = +1$ or -1). Every network activity pattern at time t was described as $V^t = [\sigma_1^t, \sigma_2^t, \cdots, \sigma_N^t]$, where N is the number of the networks (that is, N = 9, here). It should be noted that there are 2^N activity patterns in theory. According to the principle of maximum entropy, when the mean network activity $\langle \sigma_i \rangle = \frac{1}{T}\sum_{t=1}^{T}\sigma_i^t$ and the mean pairwise interactions $\langle \sigma_i \sigma_j \rangle = \frac{1}{T}\sum_{t=1}^{T}\sigma_i^t\sigma_J^t$ are constrained by the empirical data, where T is the total number of images for each network, the appearance probability $P(V_k)$ of a network activity pattern should obey a Boltzmann distribution, because such a distribution maximizes the information entropy. That is, the appearance probability should follow the formula below:

$$P(V_k) = e^{-E(V_k)} / \sum_{i=1}^{2^N} e^{-E(V_k)}$$

where

$$E(V_k) = -\sum_{i=1}^{N} h_i \sigma_i(V_k) - \frac{1}{2}\sum_{i=1}^{N}\sum_{j=1, j\neq i}^{N} J_{ij}\sigma_i(V_k)\sigma_j(V_k).$$

here, $\sigma_j(V_k)$ denotes the binarized activity of network i in activity pattern V_k, h_i represents the activation tendency of network i, and J_{ij} indicates a functional interaction between networks i and j.

Based on the $P(V_k)$, the model-based mean network activity $\langle \sigma_i \rangle_m = \sum_{l=1}^{2^N}\sigma_i(V_l)P(V_l)$ and model-based mean pairwise interactions $\langle \sigma_i\sigma_j \rangle_m = \sum_{l=1}^{2^N}\sigma_i(V_l)\sigma_j(V_l)P(V_l)$ were easy to obtain. We optimized h_i and J_{ij} by iteratively updating $\langle \sigma_i \rangle$ and $\langle \sigma_i\sigma_j \rangle$ toward $\langle \sigma_i \rangle_m$ and $\langle \sigma_i\sigma_j \rangle_m$, respectively, with a gradient ascent algorithm using the following equations,

$$h_i^{new} = h_i^{old} + \alpha_g \log \frac{\langle \sigma_i \rangle}{\langle \sigma_i \rangle_m}$$

$$J_{ij}^{new} = J_{ij}^{old} + \alpha_g \log \frac{\langle \sigma_i\sigma_j \rangle}{\langle \sigma_i\sigma_j \rangle_m}$$

The scale index α_g was initially set to 0.1. The parameters were adjusted until the gradients reached a value lower than 10^{-5}. Finally, the optimal h_i and J_{ij} for each of the healthy control and patient groups were confirmed.

To evaluate the effectiveness of the pairwise MEM, we calculated (i) a Pearson correlation coefficient between the model-based appearance probabilities and empirically obtained appearance probabilities of all the possible brain states, and (ii) the accuracy of model fitting, ACC:

$$ACC = \frac{D_1 - D_2}{D_1}$$

here,D_k is the Kullback-Leibler divergence between the probability distributions of the k-th order model network and the empirical network,

$$D_k = \sum_{l=1}^{2^N} p_N(V_l)\log_2 \frac{p_N(V_l)}{p_k(V_l)}$$

where p_N represents the empirical distribution of the network activity pattern.

2.6. Identification of local minima

The energy landscape was built and characterized as described below for each group. The energy landscape was first defined as a network of brain activity patterns $V_k(k = 1, 2, \cdots, 2^N)$ with their energy levels $E(V_k)$, in which two activity patterns were regarded as adjacent if and only if they took the opposite binary activity values at a single brain network. After that, the local minima, whose energy values were smaller than those of all the N adjacent patterns, were identified to represent the dominant brain states.

To analyze the hierarchal structures between the detected local minima, we then constructed disconnectivity graphs in the following way: (1) a local minimum was set as a node in the disconnectivity graph. All the 2^N brain activity patterns were exhaustively detected to examine whether each node was a local minimum. (2) We set a threshold energy level, denoted by E_{th}, to the largest energy level realized by (at least) one of the 2^N patterns. (3) The nodes whose energy levels were higher than E_{th} were cut. And all the links incident to a removed node were also separated. In fact, no node or link was removed when the threshold was equal to the largest possible energy level, and some nodes and links were removed by revisiting this step after lowering the threshold. (4) We judged whether each pair of local minima was connected by a path in the reduced network. In general, the local minima were classified into some connected components. (5) We repeated steps (3) (4) after moving E_{th} down to the next largest energy level realized by a node. Finally, a reduced network of the local minimum was obtained in which each local minimum was isolated. (6) On the basis of these results, a hierarchical tree-like disconnectivity graph was constructed. The terminal nodes represented the local minima and internal nodes indicated the branching points of different local minima.

2.7. Estimation of the sizes of dominant brain states

To evaluate how dominant each local minimum was, the basin size was computed for each of the detected local minimum. We randomly started from a node i belonging to the total 2^N nodes. Then, the neighbor of node i possessing the smallest energy value was identified and denoted by j. We moved to the node j if and only if any of the node j had a smaller energy value than that of node i. Otherwise, remained at the node i, node i was considered as a local minimum. We never stopped this procedure until local minima were obtained, and the starting node i was defined as a component of the basin of the local minima we finally reached. All the 2^N nodes were processed according to the above pro-

cedures. Finally, the basin of the local minima was defined as a set of the brain activity patterns belonging to the basin, and the fraction of nodes belonging to the basin was calculated to get the basin size.

2.8. Random-walk simulation of dynamics for the energy landscape

Based on the energy landscape estimated for each group, we numerically simulated the dynamics of the associated brain activity patterns by using a Markov chain Monte Carlo (MCMC) method with the Metropolis-Hastings algorithm to characterize brain dynamics. In this method, any brain activity pattern V_i is only allowed to move to its neighbring pattern V_j that is selected from all N neighbors with a uniform probability of 1/N. The probability of transition from V_i to V_j is $P_{ij} = min\left[1, e^{E(V_i)-E(V_J)}\right]$. For each group, we repeated the random walk of 10^5 steps with a randomly selected initial pattern and summarized the trajectories of the activity patterns to a series of stays and transitions among the local minima. The first 100 steps were discarded to eliminate the effects of the initial condition. Based on this numerical simulation, the transition frequency between the local minima and the duration of staying in the major states were calculated to characterize the neural dynamics.

2.9. Associations between brain dynamics and language abilities

The language abilities of the poststroke aphasia patients were measured by trained speech-language pathologists using the AAT test. Then, the language recovery scores (LRS) for language comprehension (LRS_{COMP}) and production (LRS_{PROD}) were calculated based on AAT subtests for each stage and patient, respectively. The resulting range between 0 and 1 reflected the level of rehabilitation, with a higher score representing a better degree of recovery.

We examined the associations between the changes of neural dynamics changes and the language ability scores by calculating the Pearson correlation coefficient.

2.10. Functional coordination between brain networks

Finally, to assess the ability of information processing of the whole brain, we measured the relationships between the functional coordination processes of different networks and atypical brain dynamics.

First, the strength of functional segregation between a network module (cerebellum and subcortex) and another network module (DAT, VAT, SAL, FPN, MRN, CON, and SMT) was measured, because the major state was separated into two distinct modules on the basis of segregation between these networks. Then, the strength of functional segregation was defined as the difference between the average of within-module FC and the average across-module FC based on the description of a previous study (Watanabe and Rees, 2017). For each individual, we calculated the Pearson correlation coefficient between the average network activities, that is, the global functional connectivity of nine networks we focused on. Then, the functional segregation strength was estimated according to the Fisher-transformed FC values. Finally, we inferred the relationships between this functional segregation strength, the brain dynamics and the behavioral scores.

Mathematically, if the functional interaction measured by the Pearson correlation coefficient between the brain networks i and j is sufficiently close to the pairwise interaction J_{ij} calculated by the pairwise MEM, the FC-based measurements that delineated the functional segregation strength should be highly relevant to the variability of brain dynamics (Watanabe and Rees, 2017). However, because the FC_{ij} calculated via Pearson correlation did not consider the effects of pairwise interactions, in theory, it is not equal to J_{ij}. Thus, considerable interest has been arisen with regard to examining the associations between the functional segregation processes and neural dynamics of large-scale brain networks.

2.11. Statistical tests

All correlations between the computational measures of simulated brain activity patterns including appearance probability of major states, the direct transition frequency and the major state duration and empirical measures such as the appearance frequency of brain activity patterns, the functional segregation strength and language assessment scores were obtained using Pearson correlation. All comparisons of averages between the healthy control and three phases after the left frontal stroke were done using one-way ANOVA. All comparisons of averages within aphasic group were done using repeated measure ANOVA. We built 6 repeated measure ANOVA models to test the longitudinal changes within aphasic group with every dynamic measures of simulated brain activity patterns as dependent variables and three post-stroke stages (T1, T2 and T3) were included. All results of averages comparisons were correlated for multiple comparisons using Bonferroni procedure in SPSS.

3. Results

3.1. Accuracy of model fitting

We separately analyzed the task-based fMRI data collected from the 16 patients in the acute, subacute and chronic stages after first ischemic stroke (depicted by T1, T2 and T3, respectively, in the following analysis), primarily affecting the left frontal cortex, and the 17 age-matched healthy individuals (depicted by T0 in the following analysis).

To investigate the longitudinal dynamic reorganization of different language-related subsystems during the natural recovery of poststroke aphasia patients from the acute phase to the chronic phase, the time series of average fMRI signals for each of the nine functional brain networks was extracted (Fig. 1a and 1b). Then, they were binarized according to the average value of the continuous fMRI signals of each time series (Fig. 1c), and finally we fitted a pairwise MEM to them. This model exhibited sufficiently superior performance in terms of accurately predicting the empirical data in both the stroke and healthy groups. The Pearson correlation coefficient between the simulated appearance probabilities and empirical appearance probabilities of all the possible brain states was larger than 0.93, and the accuracy index was greater than 0.83 for all the groups. (Fig. 2a).

3.2. Dominant brain states

We then proposed several dominant brain states to represent brain activity patterns during the auditory comprehension task based on the model fitted above. Typically, the dominant brain activity patterns are characterized as brain states with significantly higher observation frequencies. We calculated the energy values of all the possible brain activity patterns (2^9 patterns in theory), examined hierarchal relationships between the 2^9 energy values, and went through all the patterns to search for dominant brain states that owned the locally minimum energy values and that tended to be observed more easily than any other activity patterns.

We noted that the normal samples and different phases of stroke patients had energy landscapes with variable hierarchal structures (Fig. 2b). Specifically, the healthy group had seven local stable brain activity patterns, and the patient group exhibited six dominant patterns regardless of the stage after stroke. Although the hierarchal structures were manifold, we summarized two complementary major states (local minima A and B) in the four groups (Fig. 2c). The energy values of these two local minima were relatively low, which indicated that they were more dominant and stable than any other local minima.

It should be noted that the energy value that we are talking about here is a statistical concept, it actually indicates the appearance probability of each brain activity pattern. In short, when any activity patterns

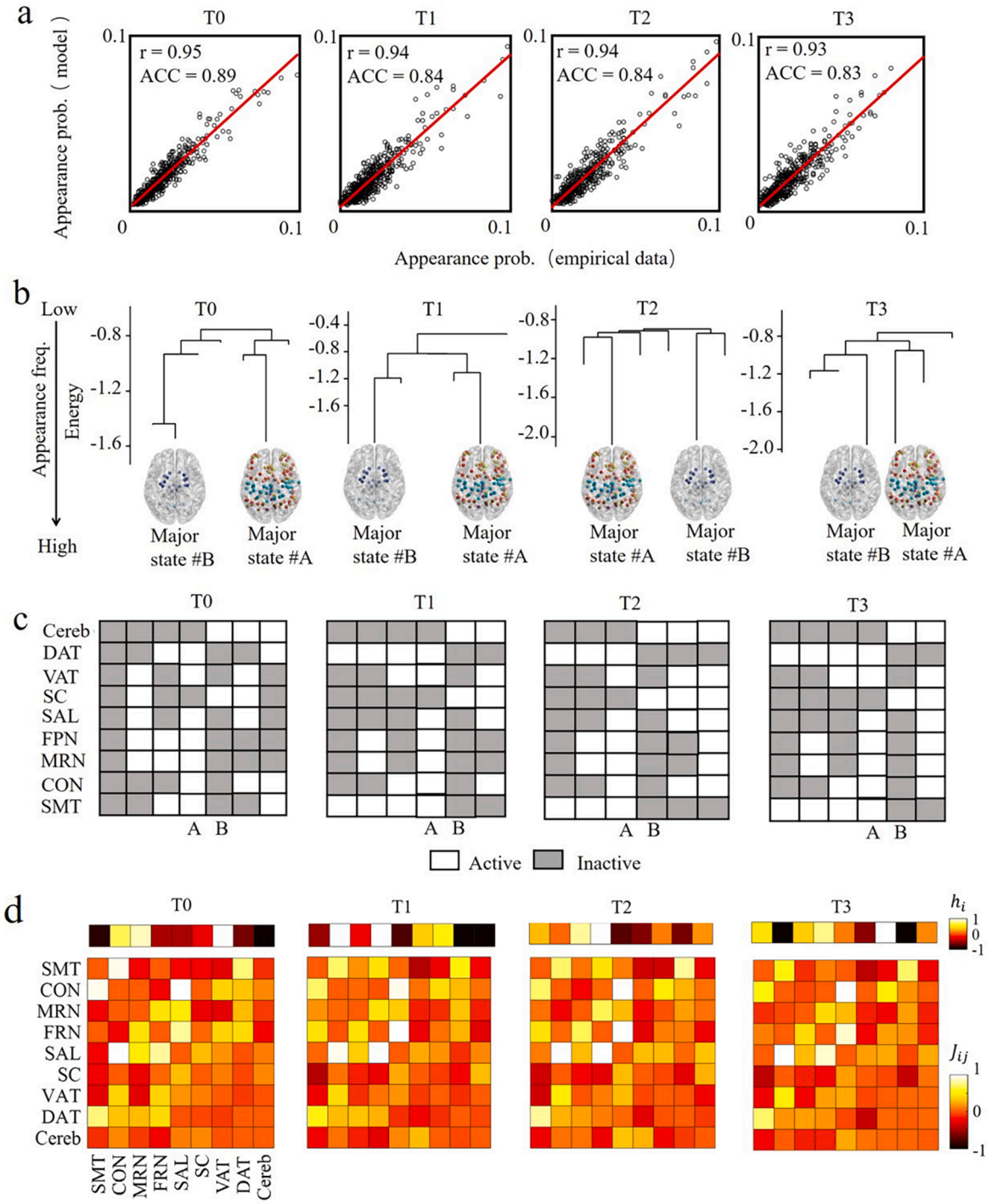

Fig. 2. Results of the pairwise MEMs fitting. In both the normal samples (T0) and three patient stages (T1, T2 and T3), the pairwise MEM showed good fitting performance and could predict appearance probability (Prob.) of brain activity patterns observed in empirical data (a). Based on the accurate fitting of pairwise MEMs, we estimated the energy values of all the 2^9 brain states and built the energy landscape for each group. Their energy landscapes exhibited different hierarchal structures (b). We then identified the dominant brain activity patterns and summarized two complementary major activity patterns in normal samples and three patient stages (local minima A and B). (c) The baseline brain activity h_i of isolated ROI and pairwise functional interations among the nine ROIs J_{ij} were calculated (d).

have lower energy values, they should be considered as stable states and be likely to appear more frequently.

3.3. Sizes of the dominant brain states

A major state is a stable brain activity pattern with a higher probability of being observed. Although both the healthy and patient groups, regardless of the time points at which we visited, had the same major

network coordination patterns, the appearance frequencies of these major states in different groups varied significantly. We calculated the dominance of the two major brain activity patterns by computing the size of each brain state, which quantified how large an area was occupied by each local minimum in an energy landscape.

In the healthy control group, the major states A and B occupied ~33 % and ~22 % of the entire energy landscape, respectively, and these two states in the patient group occupied ~40 % at the acute and subacute phases and 31 % and 32 % at the chronic phase, respectively. In particular, the frequency of major state B was significantly higher in the acute stage than in the controls ($\chi^3 = 10.19$, $P < 0.05$ in a χ^2- test; $Z = -2.8$, $P_{Bonferroni} < 0.05$ in post hoc residual tests; Fig. 3a).

The variances among the four groups were confirmed by calculating the appearance frequency of each brain state in the empirical data directly. The frequency of major state A increased significantly at the acute and subacute stages after stroke when compared to that of the healthy group ($F_{3,61} = 14.574$, $P < 0.001$ in a one-way ANOVAs, $P_{Bonferroni} < 0.05$ in post hoc tests; Fig. 3b left), and the major state B appeared more frequently at all the three patient phases than in the healthy group ($F_{3,61} = 67.387$, $P < 0.001$ in a one-way ANOVAs, $P_{Bonferroni} < 0.05$ in post hoc tests; Fig. 3b right). Longitudinally, an obvious downtrend of major state frequency occurred from acute stage to chronic stage. Both the frequency of major state A and B decreased significantly at chronic stage compared to the acute ($P_{Bonferroni} < 0.05$ in a repeated measure ANOVA, Fig. 3b) and subacute stage ($P_{Bonferroni} < 0.05$ in a repeated measure ANOVA, Fig. 3b).

Considering the variances of minor states and their relatively lower probabilities of occurrence, to simplify the descriptions, we summarized the minor brain states into one intermediate state for each group and treated them as having the same level of importance. As with the minor brain states, this intermediate state appeared less frequently in all the three phases of the patients' brains than in the controls, and the difference between the acute stage and healthy controls was significant (($\chi^3 = 23.26$, $P < 0.05$ in a χ^2- test; $Z = 3.9$, $P_{Bonferroni} < 0.05$ in post hoc residual tests; Fig. 3c). Particularly, when computed from the individual empirical data, this value decreased significantly at all of the three stages of aphasic group when compared to the healthy control ($F_{3,61} = 45.774$, $P < 0.001$ in a one-way ANOVAs, $P_{Bonferroni} < 0.05$ in post hoc tests; Fig. 3d). For aphasic group, it exhibited an obvious uptrend, which implied an alleviation of brain dysfunction. Especially, the frequency of the intermediate state at chronic phase increased significantly when compared to acute ($P_{Bonferroni} < 0.05$ in a repeated measure ANOVA; Fig. 3d) and subacute phases ($P_{Bonferroni} < 0.05$ in a repeated measure ANOVA; Fig. 3d).

The results suggest that aphasia patients who suffer a local damage in the left frontal lobe show significantly aberrant whole-brain neural

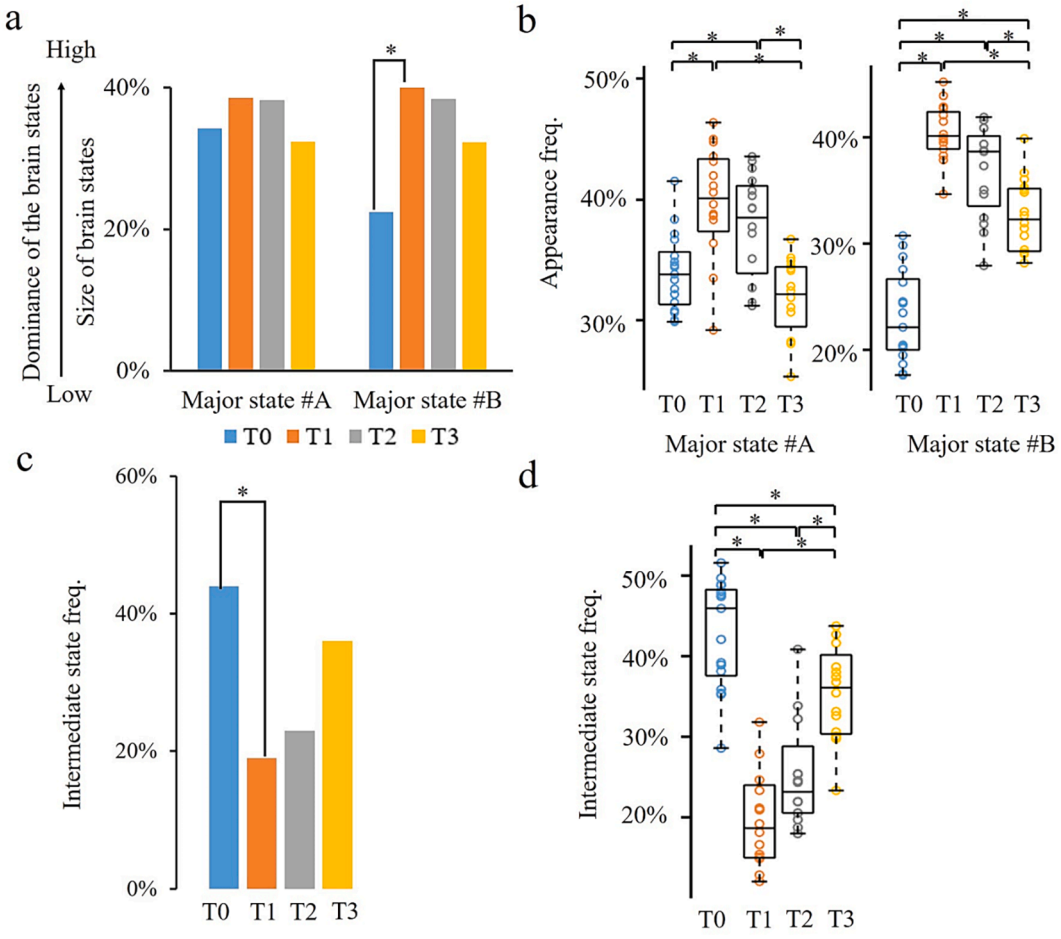

Fig. 3. Dominance of the major states (a-b) and intermediate state (c-d). The normal samples and different patient stages showed varying sizes of the major state A and B. Particularly, the size of major state B in the acute stage (T1) is significantly larger than healthy brains (T0). *$P < 0.05$ in a χ^2- test (a). Such variances of the major activity patterns were confirmed when we directly computed the sizes of the major states in the individual empirical data. The appearance frequencies of major state A and B in the acute and subacute stages were significantly larger than the healthy samples. (c) We conclude all minor states into an intermediate state and calculate the occurrence probability. The intermediate state appeared less frequently in patient groups, this difference is significant in the acute stage (c). These results were replicated in individual data (d) * between the healthy control group and aphasic group, $P_{Bonferroni} < 0.05$ in one-way ANOVA. * within aphasic group, $P_{Bonferroni} < 0.05$ in repeated measure ANOVA.

dynamics. They need to recruit the two major brain states more times to resist or attenuate the negative influence caused by local ischemic strokes and fully mobilize the whole brain functional modules comprising the cortex, subcortical structures and cerebellum to finish the tasks.

3.4. Characterization of brain dynamics

The results of basin size suggested that the patient groups recruited more major states when they executed the auditory comprehension tasks. However, it is still unclear how the major states to be recruited and what kinds of dynamic changes (trajectories) underpin such an abnormality.

To address this question, we characterized the brain dynamics as staying in, or switching among these brain states based on a 10^5-step random walk-based numerical simulation (see Methods for details) in the group-level energy landscape (Fig. 4a). To describe the micromesh neural dynamics, dynamic transitions were categorized into the following two trajectories: switches directly from one major brain state to the other and an indirect transition between the two major states via

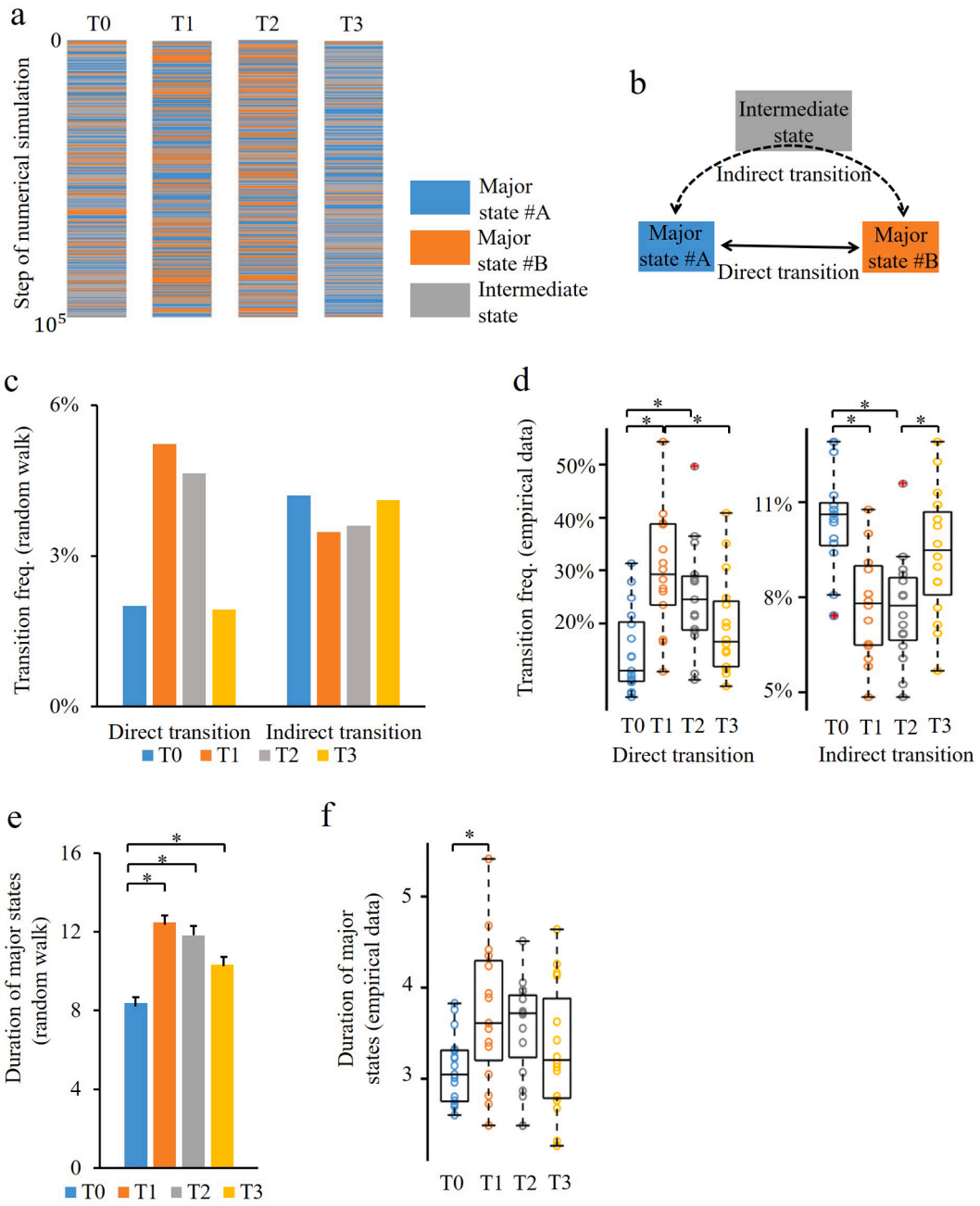

Fig. 4. Dynamics of brain activity patterns. We performed a 10^5 random-walk numerical simulation to characterize the dynamics of brain states for each of the four groups (a). Based on this simulation, we classified all transitions into two trajectories: transitions between the two major states without entering any minor state and indirectly transitions between the two major states via the intermediate state (b). There is no significant frequency difference of the two types of transitions in the simulation (c), in the empirical data, the frequencies of direct and indirect transitions in the acute and subacute phases were significantly larger than healthy samples. And the patient groups got great improvements in the chronic stage (d). The durations of the major states were significantly longer in the three patient stages in simulation (e). And we replicated such difference when it was directly computed in the empirical data, specifically, the patient in the acute phase stayed significantly longer in major states than the healthy (f). * between the healthy control group and aphasic group, $P_{Bonferroni} < 0.05$ in one-way ANOVA. * within aphasic group, $P_{Bonferroni} < 0.05$ in repeated measure ANOVA.

one of the minor states (Fig. 4b). We then counted the frequency of transitions between the two major brain activity patterns respectively and investigated the intergroup differences among the different trajectories (direct and indirect transitions). The frequencies of direct transitions between the two major states increased in all three patient phases over those of the controls (Fig. 4c, left). Adversely, the frequency of indirect transitions between the two major states decreased in all three patient phases over those of the controls (Fig. 4c, right), although they were not significant in the simulation. Following the process of rehabilitation, the major brain activity patterns switched directly and via an intermediate state at the chronic stage as frequently as in the normal group. These aberrant changes were reproduced in the individual empirical fMRI data: the direct transition frequency was significantly higher for the acute and subacute phases of the patient than for the control ($F_{3,61} = 8.038$, $P < 0.001$ in a one-way ANOVAs, $P_{Bonferroni} < 0.05$ in post hoc tests). Although the patients still needed to recruit more major states to perform the assigned task, the frequency of direct transitions decreased significantly in the chronic phase compared to that in the acute phase ($P_{Bonferroni} < 0.05$ in a repeated measure ANOVA; Fig. 4d, left). In contrast, the frequency of indirect transitions was decreased for all three patient phases. In particular, the frequency of indirect transitions for the patient group was reduced significantly compared to that of the controls at acute and subacute phases ($F_{3,61} = 8.756$, $P < 0.001$ in a one-way ANOVAs, $P_{Bonferroni} < 0.05$ in post hoc tests). As expected, the frequency of indirect transitions obviously increased relative to the former stage at chronic stage ($P_{Bonferroni} < 0.05$ in a repeated measure ANOVA; Fig. 4d, right).

Such atypically frequent direct state transitions between major states in poststroke aphasia individuals suggest that their brain dynamics are more rigid than those of the controls. This implication was confirmed by calculating how long a brain activity pattern stayed in either of the two major states. In this numerical random-walk simulation, the patients exhibited longer durations for the major states than the control group regardless of the time point of observation ($F_{3,61} = 4630$, $P < 0.001$ in a one-way ANOVAs, $P_{Bonferroni} < 0.05$ in post hoc tests; Fig. 4e). We then replicated this difference when directly counting the repetition length of the major activity patterns in the empirical data for each subject. The results showed that the difference between the acute phase and the control was significant ($F_{3,61} = 3.223$, $P < 0.05$ in a one-way ANOVA, $P_{Bonferroni} < 0.05$ in post hoc tests; Fig. 4f). There was no significant longitudinal change of the major state duration among different poststroke stages in a repeated-measure ANOVA model.

On the one hand, these results implied a passive response to the local damage, including significantly more frequent direct transitions, fewer indirect transitions between major brain activity patterns and longer durations for maintaining the major states in the acute stage. However, on the other hand, the level of neural dynamics approached normal samples at the chronic phase, suggesting the active functional reorganization of multiple large-scale brain networks.

3.5. The association between brain dynamics and language ability

Although we have found dramatic changes in the acute stage and significant improvements in the chronic stage regarding whole-brain neural dynamics, it is still indistinct whether the improvements in aberrant whole-brain dynamics support the recovery of language ability after aphasia.

To unveil this confusion, we arranged the language production and comprehension scores reported in the dataset and calculated the Pearson correlation coefficient between the neural dynamics (the frequencies of major states, the frequencies of direct/indirect transitions between the two major states and the durations of major states) and the language assessment scores for the patient group. We measured the longitudinal changes in the neural dynamics and language scores by combining the acute, subacute and chronic stages sequentially.

Patients with poststroke aphasia showed significant improvements of language production ($F_{2,45} = 13.021$, $P < 0.05$ in a Welch's ANOVA, $P_{Games-Howell} < 0.05$ in post hoc tests; Fig. 5a) and language comprehension abilities ($F_{2,45} = 18.814$, $P < 0.05$ in a Welch's ANOVA, $P_{Games-Howell} < 0.05$ in post hoc tests; Fig. 5b) in the chronic stage. We found that the frequency of major states was significantly negatively related to the language production ($r = -0.537$, $P < 0.01$; Fig. 5c) and language comprehension ($r = -0.435$, $P < 0.01$; Fig. 5d) scores. Individuals who recruited the major states more times had lower language scores, which was attributed to the abnormal turbulence of their whole-brain neural dynamics. The language connectome collapsed temporarily because of severe local damage to brain tissue. The inflexible brain organization of large-scale functional networks resulted in poor language performance at the acute stage. Following the normalization of whole-brain dynamics, the language production and comprehension abilities of patient individuals were enhanced gradually.

Relationships between brain network coordination and neural dynamics.

By inferring the energy landscape for the normal and different states of patients after stroke, we observed that the patient samples exhibited abnormal brain dynamics that were associated with an atypically larger probability of two complementary major states appearing (Fig. 6a). In other words, the patient samples exhibited overly rigid brain dynamics, which implied a decline in the flexibility of whole-brain network configurations, especially in the acute and subacute phases after stroke. We assumed that these abnormal dynamics were related to functional segregations between two different network modules (DAT/VAT/SAL/FPN/MRN/CO/SMT module (module 1) and subcortical structures/cerebellum module (module 2); Fig. 6b).

The normal group and all three patient phase groups showed significant functional segregation (the normal sample: ($t_{16} = 3.024$, $P = 0.008$), the acute phase: ($t_{15} = 5.261$, $P = 0.000096$), the subacute phase ($t_{15} = 3.233$, $P = 0.006$), and the chronic phase: ($t_{15} = 3.222$, $P = 0.006$); Fig. 6c). Furthermore, this strong functional segregation was positively correlated with the major state frequency ($r = 0.769$, $P < 0.01$; Fig. 7a1) and the frequency of direct transition ($r = 0.804$, $P < 0.01$; Fig. 7b1), but negatively correlated with the duration of staying in the major states ($r = -0.545$, $P < 0.05$; Fig. 7c1) for the normal group. Similarly, the duration of staying in the major states was significantly negatively correlated with the strength of functional segregation at the acute stage ($r = -0.548$, $P < 0.05$; Fig. 7c2) and the chronic stage ($r = -0.7$, $P < 0.01$; Fig. 7c4), and the frequency of direct transition was significantly positively correlated with the functional segregation at the chronic stage ($r = 0.74$, $P < 0.01$; Fig. 7b4). These results suggest that atypically longer major state durations and overly inflexible neural dynamics are associated with the nonsynchronous functional coordination.

To investigate whether the two modules were reconfigured synchronously or not, we investigated the relationship between the strength of functional segregation and the global functional connectivity between these large-scale brain networks. In the healthy group, we obtained a significant positive correlation between them ($r = 0.824$, $P < 0.01$; Fig. 7d1), which implied a synchronous activation pattern involving these two modules (Fig. 8a), but there was no correlation between them in the acute phase ($r = 0.127$, $P = 0.641$; Fig. 7d2) and subacute phase ($r = 0.277$, $P = 0.298$; Fig. 7d3). For the last observed stage, the strength of functional segregation still did not show a significant correlation with the global functional connectivity ($r = 0.475$, $P = 0.063$; Fig. 7d4), indicating their heterochronous oscillation during the task (Fig. 8b).

The communication between the two modules decreased due to global disturbance, which was a response to local damage. During the spontaneous recovery process, patients' brain dynamics returned basics (relatively lower major state frequencies and shorter duration of staying in major states) by decreasing the direct transition between the two major activity patterns.

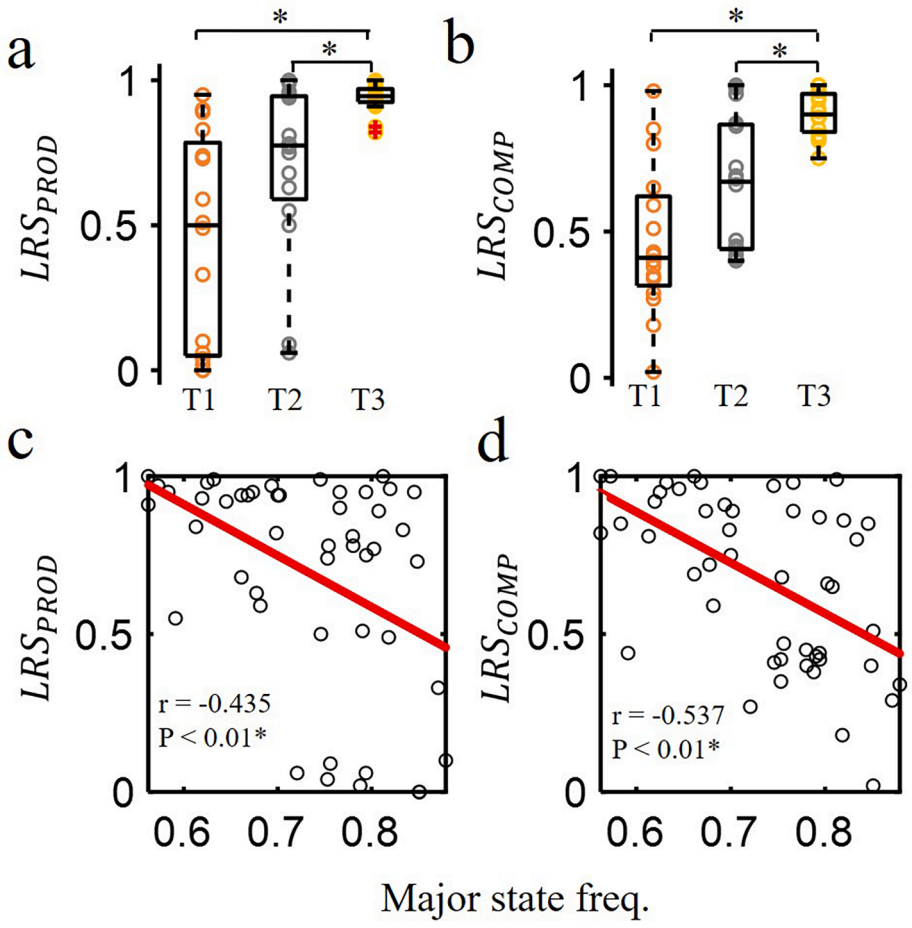

Fig. 5. The longitudinal changes of language assessment scores and brain dynamics. Both language production ability (a) and language comprehension ability (b) got significant improvements when compared to that of the former stage. * $P_{\text{Games–Howell}} < 0.05$ in Welch's ANOVA. Longitudinal observations showed that the major state frequencies were negative predictor of language production (c) and comprehension scores (d).

3.6. Dynamics of the subcortex and cerebellum systems after stroke.

Although, we observed that the appearance frequencies of both modules 1 and 2 increased aberrantly during the acute and subacute stages after stroke when compared with those of the normal samples (Fig. 3a, 3b and 6d). We also found that the subcortex and cerebellum language systems were recruited disproportionately when the brain suffered focal damage. As shown in Fig. 6d, the frequency of module 2 was significantly lower than that of module 1 for the healthy group ($t_{32} = 8.369$, $P < 0.001$). However, when the brain suffered an emergency, such as a dramatic disturbance to the large-scale networks caused by a left frontal stroke, the frequency of module 2 was close to that of module 1. We compared the frequencies of modules 1 and 2 for different stages after a stroke and found that module 2 appeared as frequently as module 1. Furthermore, the dynamics of the cerebral functional networks were close to those of normal subjects (Fig. 3b, left), but the dynamics of module 2 were significantly abnormal in the chronic stage when compared to those of the normal sample (Fig. 3b, right).

This result implied that the communication between cerebral functional systems and cerebellar/subcortical systems was increased by significantly increasing the direct transitions between two major states at the acute stage. As long as the emergency was solved or alleviated by means of functional reorganization between two modules during the subacute and chronic stages, direct communication between the two modules decreased to the basis.

4. Discussion

In the present research, we studied the neural dynamics of large-scale functional brain networks (systems) by conducting an energy landscape analysis of the aphasia brain. Our goal was to delineate the aberrant whole-brain neural dynamics of poststroke aphasia patients at different stages and track the longitudinal large-scale brain network dynamic changes during natural recovery from the acute stage to the chronic stage after a stroke. Our main findings are reported as follows. First, poststroke aphasia patients exhibited abnormal whole-brain functional system dynamics (referring to the cerebral cortex and subcortical/cerebellar structures). Second, the brains of aphasia patients were rigid, and they were restricted to two major stable states to relieve the global neural perturbance, especially during the acute stage, unlike the healthy controls. Third, following recovery, abnormal brain dynamics developed during the chronic stage, which implied the improvement of brain flexibility. We discuss these findings and their potential neurobiological impact in detail.

4.1. Both cerebral functional systems and subcortical/cerebellar structures exhibited aberrant neural dynamics compared to those of the normal samples.

Utilizing energy landscape analysis, we found that the poststroke aphasia samples produced larger appearance probabilities for the two major activity patterns (major states A and B) and lower occurrence frequencies for the intermediate states. These energy landscape analysis results are consistent with previous neuroimaging findings, which

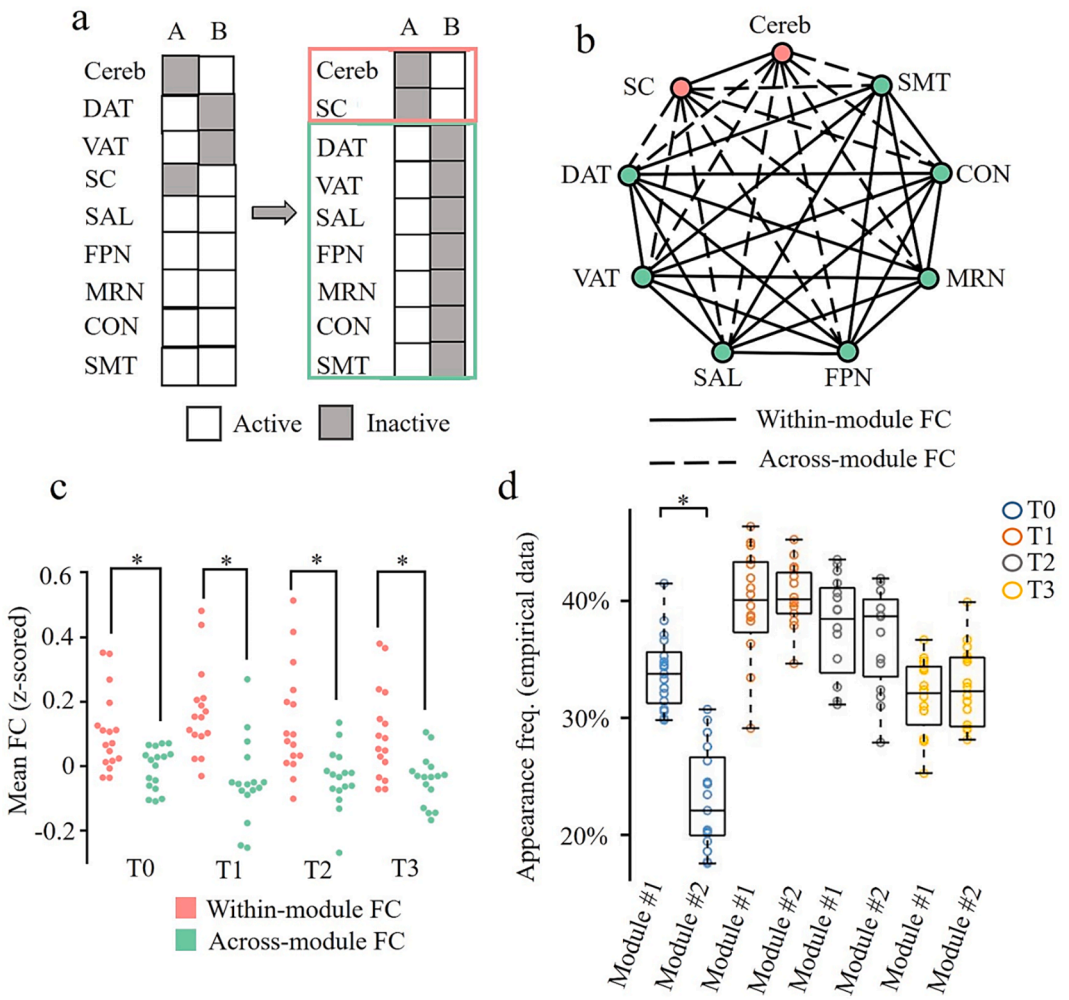

Fig. 6. Functional segregation of the large-scale brain networks during major brain states in poststroke aphasia. We proposed that two major states were driven by functional segregation between two different modules, that is, a cortex module and a subcortex/cerebellum module (a-c). The appearance frequency of module 2 was significantly smaller than module 1 in normal samples, but both module 1 and 2 appeared more frequently in the acute and subacute stages after stroke in patient group. Especially, the frequency of module 2 increased disproportionally in three patient stages (d). * $P < 0.05$ in *t*-test.

indicated that poststroke aphasia is a network disorder ascribed to multiple system abnormalities (Carter et al., 2012; Stockert and Saur, 2017; Zhu et al., 2017; Stockert et al., 2020).

Actually, both the normal sample and aphasia group possessed two types of network organization: major state A showed coordinated activity between the cerebral functional networks, including the language-specific systems and domain-general systems; major state B reflected the dynamic reorganization of the subcortical/cerebellar structures. The normal sample showed seven dominant brain states, including two major states with significantly lower probabilities of being observed than those in the acute and subacute aphasia stages and five other activity patterns with relatively low appearance frequencies compared to those of the major states. When ischemic stroke occurred in the left frontal lobe, dramatic local damage resulted in significant global dynamic perturbations. Such significant whole-brain dynamics perturbations (referring to cerebral functional systems and subcortical/cerebellar systems) especially appeared at the acute and subacute stages. As the results showed, seven nonoverlapping large-scale networks were activated synchronously in major state A. This process may be related to 1) the activation of remaining, undamaged perilesional areas (Fridriksson et al., 2010; Fridriksson et al., 2012; Thiel et al., 2013; Griffis et al., 2017), 2) the activation of contralateral lesion-homologue regions (Winhuisen et al., 2007; Turkeltaub et al., 2012; Meltzer et al., 2013; Xing et al., 2016; Kourtidou et al., 2021), 3) the participation of multidemand bilateral domain-general networks (Brownsett et al., 2014; Geranmayeh et al., 2017; Hartwigsen and Saur, 2019; Stockert et al., 2020), and 4) the important mentioned dynamical hierarchical reorganization between these areas (Saur et al., 2006; Hartwigsen and Saur, 2019; Stockert et al., 2020; Wilson and Schneck, 2021). And the cerebellum and subcortical structures were activated synchronously in major state B. These results emphasize the importance of subcortical and cerebellar systems. This is not surprising, as an increasing number of studies have focused on the activation of subcortical/cerebellar structures and emphasized that the subcortical structures may participate in the language processing by means of various cortico-subcortical connections (Broser et al., 2012; Herbet et al., 2016; Chouiter et al., 2016). A few studies have found that the basal ganglia and the cortico-subcortical networks manifest in tasks designed for language function (Ketteler et al., 2008; Ketteler et al., 2014). A recent study demonstrated that there are direct structural connections between the thalamus and Broca's area and suggested that this cortico-subcortical network is involved in language processing (Bohsali et al., 2015). Even earlier, Ullman and colleagues has inferred the existence of a basal ganglia-thalamocortical loop, in which Broca's area is a station of information acceptance and feedback (Ullman, 2006). The cerebellum may contribute to the word generation, semantic processing and sentence processing via specific cerebellocortical circuits (Argyropoulos, 2016; Moberget et al., 2016; Schwartze and Kotz, 2016; Cho et al., 2022; Geva

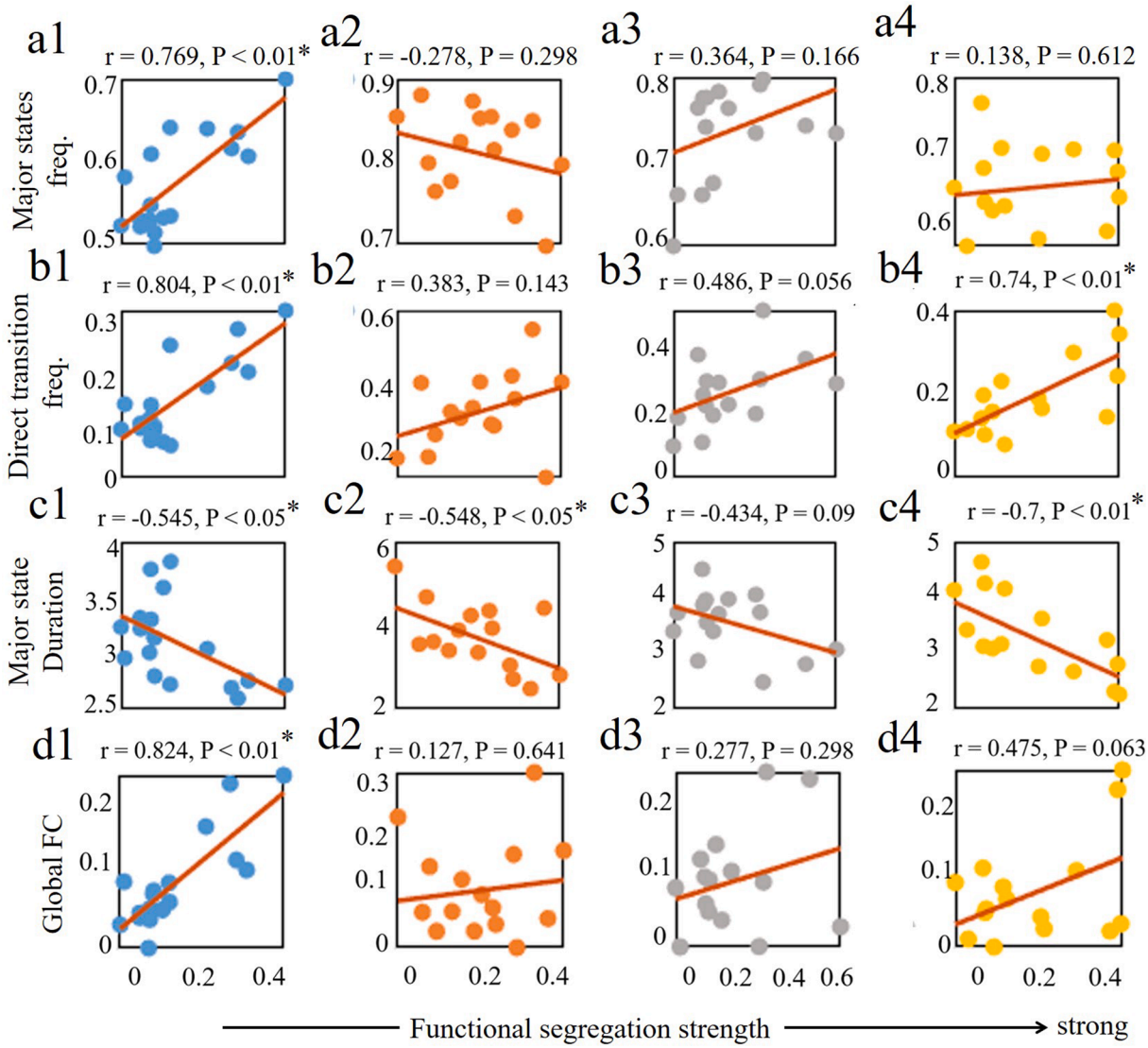

Fig. 7. The relationship between the strength of functional segregation and major state frequency (a1-a4), the frequency of direct transition (b1-b4), the duration of staying in major state (c1-c4) and the global functional connectivity (d1-d4).

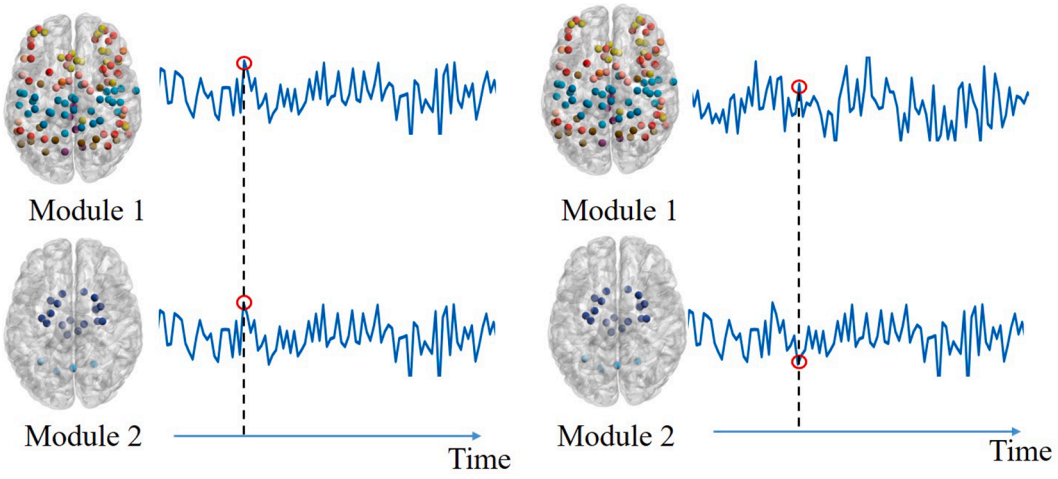

Fig. 8. Synchronous activity of two modules (a) and asynchronous activity of two modules (b).

et al., 2021).meta-analyses have demonstrated significant activation of the right posterior cerebellum during a set of language tasks (Stoodley and Schmahmann, 2009; E et al., 2014).

Obviously, the classic mode of language organization is deficient. Modern views suggest a distributed yet coordinated language connectome comprising cortical, subcortical and cerebellar areas (Dick et al., 2014; Tremblay and Dick, 2016; Fiez, 2016). Language-dominant networks need to coordinate with other systems, such as the domain-general system and subcortical/cerebellar language system, to establish a complex language connectome. Siegel et al., (Siegel et al., 2016) has reported that the post-stroke regeneration of higher cognitive functions including attention, memory and language rely on the communication between several large-scale functional networks. So, it's not surprising that most of the cognitive resources were recruited by major states to perform the language task and the frequencies of major states increased. The behavioral adaption of distinct functional networks also could be interpreted using the "neural multi-functionality", which denotes a complex neural network. The "neural multi-functionality" contributed to spontaneous recovery from post-stroke aphasia because of their constant and dynamic interaction (Cahana-Amitay and Albert, 2015).

But it's interesting that the cerebellum and subcortical structures were recruited disproportionately when the brain suffered focal damage. For comparison, we considered the dynamics of normal sample as a baseline in which the major state B could be observed relatively fewer times. Once the brain had a focal stroke, the activity pattern of major state B was reconfigured to an odd state, that is, the cerebellum and subcortical structures were activated as frequent as cerebral functional systems. The dynamics difference of cerebral system and cerebellum/subcortical structures may be related to 1) subcortical and cerebellar structures are cytoarchitectonically much denser in neural bodies than cortical regions (Hirano, 2018; Beckinghausen and Sillitoe, 2019). 2) the cerebral cortex connectome has relatively abundant modular structures (Sporns and Betzel, 2016; Newman, 2004; Betzel et al., 2018) than functional cerebellar connectome, the latter was reported to have three modular structures (Stoodley et al., 2012; Stoodley and Schmahmann, 2009; Chen et al., 2022). 3) for the above two structural bases, we can infer that the flexibility of the cerebellum/subcortical structures were limited. But further neuroimage and neurocomputational studies need to be conducted to investigate the differences of cerebral dynamics and cerebellar/subcortical dynamics, as well as the neural basis of these differences.

4.2. The aphasia samples worked in a rigid configuration to relieve or resist the global neural perturbance.

The energy landscape of the dynamic brain is comprised of several basins with local minima, whose energy values are larger than those of their neighbors in the same basin; thus, they are observed more frequently. Brain dynamics can be separated into wandering within a basin of local minima and transitions between local minima. In the latter case, a state must surpass an energy barrier. For switching between two stable states, the trajectories can be divided into direct transitions and indirect transitions. In contrast to the neural dynamics in the normal samples, the aphasia group exhibited a significantly higher direct transition frequency, a lower probability of transitions via an intermediate state and a longer duration of maintaining major activity patterns, especially for the acute stage. Notably, following the global perturbation resulting from local damage, the brain frequently wandered within and across two stable states.

Generally, the brain can maintain a basic network configuration (Cole et al., 2014; Xu et al., 2021; Pezzulo et al., 2021). When a task must be solved, the brain can communicate and reorganize itself dynamically between different large-scale networks depending on the requirements of different cognitive tasks by spontaneously modulating a small part of the network parameters (Yang et al., 2019; Zhu et al., 2020). These low-energy local minima with relatively small basin sizes can be intermediate states. They may play a vital role in fast communications between dominant attractors with high-energy and larger basin sizes by decreasing the energy barriers among these local minima (Kang et al., 2017). The occurrence probabilities of relatively low-energy local minima decreased significantly in the acute stage, which further resulted in a rigid whole brain network configuration. These results were consistent with recent studies of distributed brain networks. They reported the reduction of network modularity is a common phenotype of stroke brain (Siegel et al., 2018) including reduction of inter-hemisphere homotopic integration and within-hemisphere segregation between distinct functional systems compared to healthy brain (Siegel et al., 2017). The decreased modularity further affects the flexible interact of widely distributed cortical and subcortical functional systems (Siegel et al., 2018).

The lower occurrence probabilities of the intermediate states and the larger basin sizes of the major states resulted in longer durations of staying in major states. In addition, aphasia patients showed a significantly larger probability of direct transitions between two major states than normal samples. The brain was restricted to oscillate between these states. Such a rigid brain activity pattern is not limited to poststroke aphasia but has been reported in autism patients in recent energy landscape analyses. Watanabe and colleagues found that the brains of autism patients exhibited overly inflexible neural dynamics regarding the frequency of direct transitions between major activity patterns and the dwell time in specific major states (Watanabe and Rees, 2017). Moreover, the impaired brain network flexibility has been reported in motor deficits following stroke (Lariviere, Ward, and Boudrias, 2018). Researchers proposed that the aberrant dynamic switching of functional resources could be ascribed to the preferential allocation to the motor network during hand movements. Thus, our results suggest that preferential assignment of functional modules to language networks during short sentence comprehension task may weaken their ability to flexibly traverse from one network to another. Actually, such inflexible neural dynamics may be a defense mechanism that decreases the probability of additional perturbations introduced by external stimulation. The brain networks models of post-stroke aphasia may be a promising tool to explore it. The Virtual Brain cloud service (Schirner et al., 2022) has provide an open source framework to model brain dynamics after brain lesions (Radwan et al., 2021; Aerts et al., 2020).

4.3. The brain flexibility improved in the chronic stage.

As the results showed, we observed six to seven brain states, with two complementary major states appearing more frequently than the intermediate states. We also observed that temporally the aphasia brains traversed among nondominant states with less frequency but frequently switched back and forth between these two major activity patterns. During the chronic stage, brain flexibility improved with a lower frequency of switching between the two major states, a larger occurrence probability for the intermediate states and a shorter duration of staying in major states than during the acute stage. These results suggested that early aphasia can be characterized by the inability to flexibly switch between distinct network activation patterns (Guo et al., 2019). Following the reorganization of brain functional modules, the patients showed more varied brain activation patterns, potentially reflecting the recuperative flexibility of large-scale brain networks.

Network neuroscience has uncovered that the dynamic and flexible balance of multiple functional systems involving unimodal and transmodal large-scale networks underlines the optimal brain organization (Bressler and Menon, 2010; Margulies et al., 2016). Dynamic changes in network flexibility have been investigated during the long-term (six weeks) (Reddy et al., 2018) learning of motor skills. As learning progresses, the occurrence frequency of flexible switching among primary states and less common states increased, which imply that the cognitive resources have greater freedom to take part in other processes. Even

during short-term (five days) (Bassett et al., 2011) motor-skill learning, the brain flexibility (functional modular organization) changes over time. Compared to previous findings, our study demonstrated the longitudinally varied flexibility of large-scale networks in poststroke aphasia patients. As spontaneous recovery progresses, flexible switching among two major states and other intermediate states becomes more frequent, especially at the chronic stage. The changes of brain flexibility may be a biomarker of brain function reorganization, which need further investigation in language and other brain functions.

Limitations and challenges.

Whole-brain neural dynamics perturbations in poststroke aphasia patients were demonstrated in the current study, but there are several limitations and challenges that need to be solved in future studies. It should be firstly emphasized that we just reported the abnormal whole brain neural dynamics of the left-frontal-stroke aphasia patients and demonstrated the excellent role of energy landscape analysis for profoundly understanding the pathological mechanisms of poststroke aphasia. We can't generalize these findings to more general contexts without further studies on any kinds of post-stroke aphasia. Previous neuroimaging studies have reported the distinct recovery process after left-frontal-stroke and left temporo-parietal lesion (Stockert et al., 2020), the heterogeneous lesion locations may introduce different effects on undamaged network integration and the aphasia recovery dynamics (Siegel et al., 2018).We investigated whole-brain neural dynamics and demonstrated that aberrantly disturbed brain dynamics in aphasia patients were underpinned by the dynamic reconfiguration of two different modules involving cerebral systems and subcortical/cerebellar systems. However, what responsibilities or functions the two modules possess and how these large-scale functional networks couple or activate synchronously need further investigation. Otherwise, we inferred that inflexible neural dynamics at the acute stage may be a defense mechanism to prevent a damaged brain from additional perturbations introduced by metastable brain activity patterns. However, the specific neural pathways underlying traversal among these brain states need to be explored in future studies. Finally, like any brain state analysis with temporally coarse BOLD fMRI, although the energy landscape analysis could extract a low dimensional dynamic to make it possible to comprehend the complex system-level brain dynamics, we should be careful to conclude that there exist only a few dominant brain states in the brain. Together, these findings provide us with a new perspective to understand the damage and reorganization mechanisms of language function after strokes. They might open new opportunities for computational neuroscience-motivated language rehabilitation prescriptions. The use of a whole-brain model to characterize healthy and abnormal brain dynamic landscapes and predict potential perturbations that can switch the dynamic landscapes of patients into the desired target brain states of healthy individuals with noninvasive stimulation is an attractive topic for future study.

5. Conclusion

In summary, our analysis demonstrated that both left-frontal-stroke aphasia patients and healthy individuals exhibited two stable activity patterns during the assigned task. However, the large-scale network dynamics of patients were perturbed significantly in the acute stage, which implied the constrained, low-dimensional nature of brain dynamics in patients with acute aphasia due to left frontal lesion. Following the spontaneous recovery process, brain flexibility improved gradually. Consequently, left-frontal-lesion-induced aphasia could be characterized as less constrained, high-dimensional neural dynamics at chronic stage. This neural dynamic approach is likely to provide a new perspective for understanding the abnormal brain systems observed after strokes and the mechanism of language function recovery after stroke aphasia.

6. Data and code availability statement

We used fMRI data and behavioral assessment scores that were collected from a poststroke aphasia group and age-matched healthy group to estimate the pairwise MEM model. The patient samples were scanned and assessed in the acute, subacute and chronic stages, respectively and the healthy individuals were scanned only once. This data is publicly available through the figshare repository (https://doi.org/10.6084/m9.figshare.7093481).

7. Code availability

The code that we used in this study is available from the author for reasonable request.

8. Data for reference

The functional MRI data and relevant behavioral data used in this study can be found in the figshare repository (https://doi.org/10.6084/m9.figshare.7093481).

CRediT authorship contribution statement

Liming Fan: Conceptualization, Data curation, Formal analysis, Investigation, Methodology, Visualization, Writing – original draft, Writing – review & editing. **Chenxi Li:** Data curation, Formal analysis, Methodology, Writing – review & editing. **Zi-gang Huang:** Methodology, Writing – review & editing. **Jie Zhao:** Writing – review & editing. **Xiaofeng Wu:** Writing – review & editing. **Tian Liu:** Methodology, Writing – review & editing. **Youjun Li:** Supervision, Funding acquisition, Methodology, Writing – review & editing. **Jue Wang:** Supervision, Conceptualization, Funding acquisition, Project administration, Resources, Writing – review & editing.

Declaration of Competing Interest

The authors declare that they have no known competing financial interests or personal relationships that could have appeared to influence the work reported in this paper.

Data availability

I have shared the link of my data in the manuscript and I have stated that the code will be made available under reasonable request.

Acknowledgments

This work was supported by the National Natural Science Foundation of China (Grant No. 31972907), National Natural Science Foundation of China (Grant No. 61431012), National Key R&D Program Project (Grant No. 2021YFC2400203), Natural Science Basic Research Program of Shaanxi (Program No.2020JQ-096).

Appendix A. Supplementary data

Supplementary data to this article can be found online at https://doi.org/10.1016/j.nicl.2022.103190.

References

Ackermann, H., 2013. The contribution of the cerebellum to speech and language. Brain Lang. 127, 315–316. https://doi.org/10.1159/000102928.

Aerts, H., Schirner, M., Dhollander, T., Jeurissen, B., Achten, E., Van Roost, D., Ritter, P., Marinazzo, D., 2020. Modeling brain dynamics after tumor resection using The Virtual Brain. Neuroimage 213, 116738. https://doi.org/10.1016/j.neuroimage.2020.116738.

Argyropoulos, G.P., 2016. The cerebellum, internal models and prediction in 'non-motor' aspects of language: A critical review. Brain Lang. 161, 4–17. https://doi.org/10.1016/j.bandl.2015.08.003.
Ashida, R., N. L. Cerminara, R. J. Edwards, R. Apps, and J. C. W. Brooks. 2019. 'Sensorimotor, language, and working memory representation within the human cerebellum', 40: 4732-47. https://doi.org/10.1002/hbm.24733.
Ashourvan, A., Gu, S., Mattar, M.G., Vettel, J.M., Bassett, D.S., 2017. The energy landscape underpinning module dynamics in the human brain connectome. Neuroimage 157, 364–380. https://doi.org/10.1016/j.neuroimage.2017.05.067.
Bassett, D.S., Wymbs, N.F., Porter, M.A., Mucha, P.J., Carlson, J.M., Grafton, S.T., 2011. Dynamic reconfiguration of human brain networks during learning. Proc. Natl. Acad. Sci. U.S.A. 108, 7641–7646. https://doi.org/10.1073/pnas.1018985108.
Beckinghausen, J., Sillitoe, R.V., 2019. Insights into cerebellar development and connectivity. Neurosci Lett 688, 2–13. https://doi.org/10.1016/j.neulet.2018.05.013.
Betzel, R.F., Medaglia, J.D., Bassett, D.S., 2018. Diversity of meso-scale architecture in human and non-human connectomes. Nat. Commun. 9, 346. https://doi.org/10.1038/s41467-017-02681-z.
Bohsali, A.A., Triplett, W., Sudhyadhom, A., Gullett, J.M., McGregor, K., FitzGerald, D.B., Mareci, T., White, K., Crosson, B., 2015. Broca's area - thalamic connectivity. Brain Lang. 141, 80–88. https://doi.org/10.1016/j.bandl.2014.12.001.
Branco, P., D. Seixas, and S. L. Castro. 2020. 'Mapping language with resting-state functional magnetic resonance imaging: A study on the functional profile of the language network', 41: 545-60. https://doi.org/10.1002/hbm.24821.
Bressler, S.L., Menon, V., 2010. Large-scale brain networks in cognition: emerging methods and principles. Trends Cogn. Sci. 14, 277–290. https://doi.org/10.1016/j.tics.2010.04.004.
Broser, P.J., Groeschel, S., Hauser, T.K., Lidzba, K., Wilke, M., 2012. Functional MRI-guided probabilistic tractography of cortico-cortical and cortico-subcortical language networks in children. Neuroimage 63, 1561–1570. https://doi.org/10.1016/j.neuroimage.2012.07.060.
Brownsett, S.L., Warren, J.E., Geranmayeh, F., Woodhead, Z., Leech, R., Wise, R.J., 2014. Cognitive control and its impact on recovery from aphasic stroke. Brain 137, 242–254. https://doi.org/10.1093/brain/awt289.
Cahana-Amitay, D., Albert, M.L., 2015. Neuroscience of aphasia recovery: the concept of neural multifunctionality. Curr. Neurol. Neurosci. Rep. 15, 41. https://doi.org/10.1007/s11910-015-0568-7.
Carter, A.R., Shulman, G.L., Corbetta, M., 2012. Why use a connectivity-based approach to study stroke and recovery of function? Neuroimage 62, 2271–2280. https://doi.org/10.1016/j.neuroimage.2012.02.070.
Chao-Gan, Y., Yu-Feng, Z., 2010. DPARSF: A MATLAB toolbox for "pipeline" data analysis of resting-state fMRI. Front. Syst. Neurosci. 4, 13. https://doi.org/10.3389/fnsys.2010.00013.
Chen, Y.A., Huang, T.R., 2017. Multistability of the brain network for self-other processing. Sci. Rep. 7, 43313. https://doi.org/10.1038/srep43313.
Chen, Z., Zhang, R., Huo, H., Liu, P., Zhang, C., Feng, T., 2022. Functional connectome of human cerebellum. Neuroimage 251, 119015. https://doi.org/10.1016/j.neuroimage.2022.119015.
Chenery, H.J., Copland, D.A., Murdoch, B.E., 2002. Complex language functions and subcortical mechanisms: evidence from Huntington's disease and patients with non-thalamic subcortical lesions. Int. J. Lang. Commun. Disord. 37, 459–474. https://doi.org/10.1080/1368282021000007730.
Cho, N.S., Peck, K.K., Gene, M.N., Jenabi, M., Holodny, A.I., 2022. Resting-state functional MRI language network connectivity differences in patients with brain tumors: exploration of the cerebellum and contralesional hemisphere. Brain Imaging Behav. 16 (1), 252–262.
Chouiter, L., Holmberg, J., Manuel, A.L., Colombo, F., Clarke, S., Annoni, J.M., Spierer, L., 2016. Partly segregated cortico-subcortical pathways support phonologic and semantic verbal fluency: A lesion study. Neuroscience 329, 275–283. https://doi.org/10.1016/j.neuroscience.2016.05.029.
Cignetti, F., Nemmi, F., Vaugoyeau, M., Girard, N., Albaret, J.M., Chaix, Y., Peran, P., Assaiante, C., 2020. Intrinsic cortico-subcortical functional connectivity in developmental dyslexia and developmental coordination disorder. Cereb. Cortex Commun. 1, tgaa011. https://doi.org/10.1093/texcom/tgaa011.
Cole, M.W., Bassett, D.S., Power, J.D., Braver, T.S., Petersen, S.E., 2014. Intrinsic and task-evoked network architectures of the human brain. Neuron 83, 238–251. https://doi.org/10.1016/j.neuron.2014.05.014.
Copland, D., 2003. 'The basal ganglia and semantic engagement: potential insights from semantic priming in individuals with subcortical vascular lesions Parkinson's disease, and cortical lesions. *J. Int. Neuropsychol. Soc.* 9, 1041–1052. https://doi.org/10.1017/s1355617703970081.
Crosson, B., 1985. Subcortical functions in language: a working model. Brain Lang. 25, 257–292. https://doi.org/10.1016/0093-934x(85)90085-9.
Deco, G., Jirsa, V.K., 2012. Ongoing cortical activity at rest: criticality, multistability, and ghost attractors. J. Neurosci. 32, 3366–3375. https://doi.org/10.1523/JNEUROSCI.2523-11.2012.
Deco, G., Jirsa, V.K., McIntosh, A.R., 2013. Resting brains never rest: computational insights into potential cognitive architectures. Trends Neurosci. 36, 268–274. https://doi.org/10.1016/j.tins.2013.03.001.
Dick, A.S., Bernal, B., Tremblay, P., 2014. The language connectome: new pathways, new concepts. Neuroscientist 20, 453–467. https://doi.org/10.1177/1073858413513502.
Ding, J., Martin, R.C., Hamilton, A.C., Schnur, T.T., 2020. Dissociation between frontal and temporal-parietal contributions to connected speech in acute stroke. Brain 143, 862–876. https://doi.org/10.1093/brain/awaa027.
Duff, M.C., Covington, N.V., Hilverman, C., Cohen, N.J., 2019. Semantic memory and the hippocampus: revisiting, reaffirming, and extending the reach of their critical relationship. Front. Hum. Neurosci. 13, 471. https://doi.org/10.3389/fnhum.2019.00471.
Duncan, E.S., Small, S.L., 2018. Changes in dynamic resting state network connectivity following aphasia therapy. Brain Imaging Behav. 12, 1141–2119. https://doi.org/10.1007/s11682-017-9771-2.
E, K.-H., Chen, S.-H., Ho, M.-H., Desmond, J.E., 2014. A meta-analysis of cerebellar contributions to higher cognition from PET and fMRI studies. Hum. Brain Mapp. 35 (2), 593–615.
Ezaki, T., Watanabe, T., Ohzeki, M., Masuda, N., 2017. Energy landscape analysis of neuroimaging data. Philos. Trans. A Math. Phys. Eng. Sci. 375 (2096), 20160287.
Fedorenko, E., Thompson-Schill, S.L., 2014. Reworking the language network. Trends Cogn. Sci. 18, 120–126. https://doi.org/10.1016/j.tics.2013.12.006.
Fiez, J.A., 2016. The cerebellum and language: Persistent themes and findings. Brain Lang. 161, 1–3. https://doi.org/10.1016/j.bandl.2016.09.004.
Flowers, H. L., S. A. Skoretz, F. L. Silver, E. Rochon, J. Fang, C. Flamand-Roze, and R. Martino. 2016. Poststroke aphasia frequency, recovery, and outcomes: a systematic review and meta-analysis, *Arch Phys. Med. Rehabil.*, 97: 2188-201.e8. https://doi.org/10.1016/j.apmr.2016.03.006.
François, C., and P. Ripollés. 2019. Right structural and functional reorganization in four-year-old children with perinatal arterial ischemic stroke predict language production, 6. https://doi.org/10.1523/eneuro.0447-18.2019.
Freyer, F., Roberts, J.A., Becker, R., Robinson, P.A., Ritter, P., Breakspear, M., 2011. Biophysical mechanisms of multistability in resting-state cortical rhythms. J. Neurosci. 31, 6353–6361. https://doi.org/10.1523/JNEUROSCI.6693-10.2011.
Fridriksson, J., Bonilha, L., Baker, J.M., Moser, D., Rorden, C., 2010. Activity in preserved left hemisphere regions predicts anomia severity in aphasia. Cereb. Cortex 20, 1013–1019. https://doi.org/10.1093/cercor/bhp160.
Fridriksson, J., Richardson, J.D., Fillmore, P., Cai, B., 2012. Left hemisphere plasticity and aphasia recovery. Neuroimage 60, 854–863. https://doi.org/10.1016/j.neuroimage.2011.12.057.
Geranmayeh, F., Wise, R.J., Mehta, A., Leech, R., 2014. Overlapping networks engaged during spoken language production and its cognitive control. J. Neurosci. 34, 8728–8740. https://doi.org/10.1523/jneurosci.0428-14.2014.
Geranmayeh, F., Chau, T.W., Wise, R.J.S., Leech, R., Hampshire, A., 2017. Domain-general subregions of the medial prefrontal cortex contribute to recovery of language after stroke. Brain 140, 1947–1958. https://doi.org/10.1093/brain/awx134.
Gerstenecker, A., Lazar, R.M., 2019. Language recovery following stroke. Clin. Neuropsychol. 33, 928–947. https://doi.org/10.1080/13854046.2018.1562093.
Geva, S., Schneider, L.M., Roberts, S., Green, D.W., Price, C.J., 2021. The effect of focal damage to the right medial posterior cerebellum on word and sentence comprehension and production. Front. Hum. Neurosci. 15, 664650 https://doi.org/10.3389/fnhum.2021.664650.
Griffis, J.C., Nenert, R., Allendorfer, J.B., Vannest, J., Holland, S., Dietz, A., Szaflarski, J. P., 2017. The canonical semantic network supports residual language function in chronic post-stroke aphasia. Hum. Brain Mapp. 38, 1636–1658. https://doi.org/10.1002/hbm.23476.
Gu, S., Cieslak, M., Baird, B., Muldoon, S.F., Grafton, S.T., Pasqualetti, F., Bassett, D.S., 2018. The energy landscape of neurophysiological activity implicit in brain network structure. Sci. Rep. 8, 2507. https://doi.org/10.1038/s41598-018-20123-8.
Guo, J., B. B. Biswal. 2019. Altered dynamics of brain segregation and integration in poststroke aphasia, 40: 3398-409. https://doi.org/10.1002/hbm.24605.
Hansen, E.C., Battaglia, D., Spiegler, A., Deco, G., Jirsa, V.K., 2015. Functional connectivity dynamics: modeling the switching behavior of the resting state. Neuroimage 105, 525–535. https://doi.org/10.1016/j.neuroimage.2014.11.001.
Hartwigsen, G., Saur, D., 2019. Neuroimaging of stroke recovery from aphasia - Insights into plasticity of the human language network. Neuroimage 190, 14–31. https://doi.org/10.1016/j.neuroimage.2017.11.056.
Harvey, D.Y., Podell, J., Turkeltaub, P.E., Faseyitan, O., Coslett, H.B., Hamilton, R.H., 2017. Functional reorganization of right prefrontal cortex underlies sustained naming improvements in chronic aphasia via repetitive transcranial magnetic stimulation. Cogn. Behav. Neurol. 30, 133–144. https://doi.org/10.1097/wnn.0000000000000141.
Herbet, G., Moritz-Gasser, S., Boiseau, M., Duvaux, S., Cochereau, J., Duffau, H., 2016. Converging evidence for a cortico-subcortical network mediating lexical retrieval. Brain 139, 3007–3021. https://doi.org/10.1093/brain/aww220.
Hirano, T., 2018. Purkinje neurons: development, morphology, and function. Cerebellum 17, 699–700. https://doi.org/10.1007/s12311-018-0985-7.
Kang, J., S. O. Jeong, C. Pae, and H. J. Park. 2021. Bayesian estimation of maximum entropy model for individualized energy landscape analysis of brain state dynamics, *Hum Brain Mapp*, 42: 3411-28. https://doi.org/10.1002/hbm.25442.
Kang, J., C. Pae, H. J. Park. 2017. Energy landscape analysis of the subcortical brain network unravels system properties beneath resting state dynamics, *Neuroimage*, 149: 153-64. https://doi.org/10.1016/j.neuroimage.2017.01.075.
Kapon, R., Nevo, R., Reich, Z., 2008. Protein energy landscape roughness. Biochem. Soc. Trans. 36, 1404–1408. https://doi.org/10.1042/bst0361404.
Ketteler, D., Kastrau, F., Vohn, R., Huber, W., 2008. The subcortical role of language processing. High level linguistic features such as ambiguity-resolution and the human brain; an fMRI study. Neuroimage 39, 2002–2009. https://doi.org/10.1016/j.neuroimage.2007.10.023.
Ketteler, S., Ketteler, D., Vohn, R., Kastrau, F., Schulz, J.B., Reetz, K., Huber, W., 2014. The processing of lexical ambiguity in healthy ageing and Parkinsons disease: role of cortico-subcortical networks. Brain Res. 1581, 51–63. https://doi.org/10.1016/j.brainres.2014.06.030.

Kiran, S., Thompson, C.K., 2019. Neuroplasticity of language networks in aphasia: advances, updates, and future challenges. Front. Neurol. 10, 295. https://doi.org/10.3389/fneur.2019.00295.
Klooster, N.B., Tranel, D., Duff, M.C., 2020. The hippocampus and semantic memory over time. Brain Lang. 201, 104711 https://doi.org/10.1016/j.bandl.2019.104711.
Kourtidou, E., Kasselimis, D., Angelopoulou, G., Karavasilis, E., Velonakis, G., Kelekis, N., Zalonis, I., Evdokimidis, I., Potagas, C., Petrides, M., 2021. The role of the right hemisphere white matter tracts in chronic aphasic patients after damage of the language tracts in the left hemisphere. Front. Hum. Neurosci. 15, 635750 https://doi.org/10.3389/fnhum.2021.635750.
Lariviere, S., Ward, N.S., Boudrias, M.H., 2018. Disrupted functional network integrity and flexibility after stroke: Relation to motor impairments. Neuroimage Clin. 19, 883–891. https://doi.org/10.1016/j.nicl.2018.06.010.
Margulies, D.S., Ghosh, S.S., Goulas, A., Falkiewicz, M., Huntenburg, J.M., Langs, G., Bezgin, G., Eickhoff, S.B., Castellanos, F.X., Petrides, M., Jefferies, E., Smallwood, J., 2016. Situating the default-mode network along a principal gradient of macroscale cortical organization. Proc. Natl. Acad. Sci. U.S.A. 113, 12574–21259. https://doi.org/10.1073/pnas.1608282113.
Mariën, P., Borgatti, R., 2018. Language and the cerebellum. Handb. Clin. Neurol. 154, 181–202. https://doi.org/10.1016/b978-0-444-63956-1.00011-4.
Meltzer, J.A., Wagage, S., Ryder, J., Solomon, B., Braun, A.R., 2013. Adaptive significance of right hemisphere activation in aphasic language comprehension. Neuropsychologia 51, 1248–1259. https://doi.org/10.1016/j.neuropsychologia.2013.03.007.
Moberget, T., Hilland, E., Andersson, S., Lundar, T., Due-Tonnessen, B.J., Heldal, A., Ivry, R.B., Endestad, T., 2016. Patients with focal cerebellar lesions show reduced auditory cortex activation during silent reading. Brain Lang. 161, 18–27. https://doi.org/10.1016/j.bandl.2015.08.004.
Munn, B.R., Muller, E.J., Wainstein, G., Shine, J.M., 2021. The ascending arousal system shapes neural dynamics to mediate awareness of cognitive states. Nat. Commun. 12, 6016. https://doi.org/10.1038/s41467-021-26268-x.
Murdoch, B.E., 2010. The cerebellum and language: historical perspective and review. Cortex 46, 858–868. https://doi.org/10.1016/j.cortex.2009.07.018.
Nasios, G., Dardiotis, E., Messinis, L., 2019. From broca and wernicke to the neuromodulation era: insights of brain language networks for neurorehabilitation. Behav. Neurol. 2019, 1–10.
Neelamraju, S., Gosavi, S., Wales, D.J., 2018. Energy landscape of the designed protein Top7. J. Phys. Chem. B 122, 12282–12291. https://doi.org/10.1021/acs.jpcb.8b08499.
Newman, M.E., 2004. Fast algorithm for detecting community structure in networks. Phys. Rev. E Stat. Nonlin. Soft Matter. Phys. 69, 066133 https://doi.org/10.1103/PhysRevE.69.066133.
Othayoth, R., Thoms, G., Li, C., 2020. An energy landscape approach to locomotor transitions in complex 3D terrain. Proc. Natl. Acad. Sci. U.S.A. 117, 14987–14995. https://doi.org/10.1073/pnas.1918297117.
Pezzulo, G., Zorzi, M., Corbetta, M., 2021. The secret life of predictive brains: what's spontaneous activity for? Trends Cogn. Sci. 25, 730–743. https://doi.org/10.1016/j.tics.2021.05.007.
Power, J.D., Cohen, A.L., Nelson, S.M., Wig, G.S., Barnes, K.A., Church, J.A., Vogel, A.C., Laumann, T.O., Miezin, F.M., Schlaggar, B.L., Petersen, S.E., 2011. Functional network organization of the human brain. Neuron 72, 665–678. https://doi.org/10.1016/j.neuron.2011.09.006.
Radwan, A.M., Emsell, L., Blommaert, J., Zhylka, A., Kovacs, S., Theys, T., Sollmann, N., Dupont, P., Sunaert, S., 2021. Virtual brain grafting: Enabling whole brain parcellation in the presence of large lesions. Neuroimage 229, 117731. https://doi.org/10.1016/j.neuroimage.2021.117731.
Reddy, P.G., Mattar, M.G., Murphy, A.C., Wymbs, N.F., Grafton, S.T., Satterthwaite, T.D., Bassett, D.S., 2018. Brain state flexibility accompanies motor-skill acquisition. Neuroimage 171, 135–147. https://doi.org/10.1016/j.neuroimage.2017.12.093.
Riehl, J.R., Palanca, B.J., Ching, S., 2018. High-energy brain dynamics during anesthesia-induced unconsciousness. Netw. Neurosci. 1, 431–445. https://doi.org/10.1162/NETN_a_00023.
Ross-Naylor, J.A., Mijajlovic, M., Biggs, M.J., 2020. Energy landscape mapping and replica exchange molecular dynamics of an adsorbed peptide. J. Phys. Chem. B 124, 2527–2538. https://doi.org/10.1021/acs.jpcb.9b10568.
Saur, D., Lange, R., Baumgaertner, A., Schraknepper, V., Willmes, K., Rijntjes, M., Weiller, C., 2006. Dynamics of language reorganization after stroke. Brain 129, 1371–1384. https://doi.org/10.1093/brain/awl090.
Sayal, A., Sousa, T., Duarte, J.V., Costa, G.N., Martins, R., Castelo-Branco, M., 2020. Identification of competing neural mechanisms underlying positive and negative perceptual hysteresis in the human visual system. Neuroimage 221, 117153. https://doi.org/10.1016/j.neuroimage.2020.117153.
Schirner, M., Domide, L., Perdikis, D., Triebkorn, P., Stefanovski, L., Pai, R., Prodan, P., Valean, B., Palmer, J., Langford, C., Blickensdorfer, A., van der Vlag, M., Diaz-Pier, S., Peyser, A., Klijn, W., Pleiter, D., Nahm, A., Schmid, O., Woodman, M., Zehl, L., Fousek, J., Petkoski, S., Kusch, L., Hashemi, M., Marinazzo, D., Mangin, J.F., Floel, A., Akintoye, S., Stahl, B.C., Cepic, M., Johnson, E., Deco, G., McIntosh, A.R., Hilgetag, C.C., Morgan, M., Schuller, B., Upton, A., McMurtrie, C., Dickscheid, T., Bjaalie, J.G., Amunts, K., Mersmann, J., Jirsa, V., Ritter, P., 2022. Brain simulation as a cloud service: The Virtual Brain on EBRAINS. Neuroimage 251, 118973. https://doi.org/10.1016/j.neuroimage.2022.118973.
Schwartze, M., Kotz, S.A., 2016. Contributions of cerebellar event-based temporal processing and preparatory function to speech perception. Brain Lang 161, 28–32. https://doi.org/10.1016/j.bandl.2015.08.005.
Shaw, K., Brennan, N., Woo, K., Zhang, Z., Young, R., Peck, K.K., Holodny, A., 2016. Infiltration of the basal ganglia by brain tumors is associated with the development of co-dominant language function on fMRI. Brain Lang. 155–156, 44–48. https://doi.org/10.1016/j.bandl.2016.04.002.
Shi, E.R., Zhang, Q., 2020. A domain-general perspective on the role of the basal ganglia in language and music: Benefits of music therapy for the treatment of aphasia. Brain Lang. 206, 104811 https://doi.org/10.1016/j.bandl.2020.104811.
Siegel, J. S., L. E. Ramsey, and A. Z. Snyder. 2016. 'Disruptions of network connectivity predict impairment in multiple behavioral domains after stroke', 113: E4367-76. https://doi.org/10.1073/pnas.1521083113.
Siegel, J.S., Mitra, A., Laumann, T.O., Seitzman, B.A., Raichle, M., Corbetta, M., Snyder, A.Z., 2017. Data quality influences observed links between functional connectivity and behavior. Cereb Cortex 27, 4492–4502. https://doi.org/10.1093/cercor/bhw253.
Siegel, J.S., Seitzman, B.A., Ramsey, L.E., Ortega, M., Gordon, E.M., Dosenbach, N.U.F., Petersen, S.E., Shulman, G.L., Corbetta, M., 2018. Re-emergence of modular brain networks in stroke recovery. Cortex 101, 44–59. https://doi.org/10.1016/j.cortex.2017.12.019.
Sporns, O., Betzel, R.F., 2016. Modular brain networks. Annu. Rev. Psychol. 67, 613–640. https://doi.org/10.1146/annurev-psych-122414-033634.
Stewman, S. F., K. K. Tsui, A. Ma. 2020. Dynamic instability from non-equilibrium structural transitions on the energy landscape of microtubule, *Cell Syst.*, 11: 608-24. e9. https://doi.org/10.1016/j.cels.2020.09.008.
Stockert, A., Saur, D., 2017. Aphasia: a neuronal network disorder. Nervenarzt 88, 866–873. https://doi.org/10.1007/s00115-017-0356-5.
Stockert, A., Wawrzyniak, M., Klingbeil, J., Wrede, K., Kümmerer, D., Hartwigsen, G., Kaller, C.P., Weiller, C., Saur, D., 2020. Dynamics of language reorganization after left temporo-parietal and frontal stroke. Brain 143, 844–861. https://doi.org/10.1093/brain/awaa023.
Stoodley, C.J., Schmahmann, J.D., 2009. Functional topography in the human cerebellum: a meta-analysis of neuroimaging studies. Neuroimage 44, 489–501. https://doi.org/10.1016/j.neuroimage.2008.08.039.
Stoodley, C.J., Valera, E.M., Schmahmann, J.D., 2012. Functional topography of the cerebellum for motor and cognitive tasks: an fMRI study. Neuroimage 59, 1560–1570. https://doi.org/10.1016/j.neuroimage.2011.08.065.
Thiel, A., Hartmann, A., Rubi-Fessen, I., Anglade, C., Kracht, L., Weiduschat, N., Kessler, J., Rommel, T., Heiss, W.D., 2013. Effects of noninvasive brain stimulation on language networks and recovery in early poststroke aphasia. Stroke 44, 2240–2246. https://doi.org/10.1161/STROKEAHA.111.000574.
Thiel, A., Zumbansen, A., 2016. The pathophysiology of post-stroke aphasia: A network approach. PLoS ONE 34, 507–518. https://doi.org/10.1371/journal.pone.0183349.
Tognoli, E., Kelso, J.A., 2014. The metastable brain. Neuron 81, 35–48. https://doi.org/10.1016/j.neuron.2013.12.022.
Tremblay, P., Dick, A.S., 2016. Broca and Wernicke are dead, or moving past the classic model of language neurobiology. Brain Lang. 162, 60–71. https://doi.org/10.1016/j.bandl.2016.08.004.
Turkeltaub, P.E., Coslett, H.B., Thomas, A.L., Faseyitan, O., Benson, J., Norise, C., Hamilton, R.H., 2012. The right hemisphere is not unitary in its role in aphasia recovery. Cortex 48, 1179–1186. https://doi.org/10.1016/j.cortex.2011.06.010.
Tzourio-Mazoyer, N., Landeau, B., Papathanassiou, D., Crivello, F., Etard, O., Delcroix, N., Mazoyer, B., Joliot, M., 2002. Automated anatomical labeling of activations in SPM using a macroscopic anatomical parcellation of the MNI MRI single-subject brain. Neuroimage 15, 273–289. https://doi.org/10.1006/nimg.2001.0978.
Ullman, M.T., 2006. Is Broca's area part of a basal ganglia thalamocortical circuit? Cortex 42, 480–545. https://doi.org/10.1016/s0010-9452(08)70382-4.
Vasa, F., Shanahan, M., Hellyer, P.J., Scott, G., Cabral, J., Leech, R., 2015. Effects of lesions on synchrony and metastability in cortical networks. Neuroimage 118, 456–467. https://doi.org/10.1016/j.neuroimage.2015.05.042.
Vigneau, M., Beaucousin, V., Herve, P.Y., Duffau, H., Crivello, F., Houde, O., Mazoyer, B., Tzourio-Mazoyer, N., 2006. Meta-analyzing left hemisphere language areas: phonology, semantics, and sentence processing. Neuroimage 30, 1414–1432. https://doi.org/10.1016/j.neuroimage.2005.11.002.
Vigneau, M., Beaucousin, V., Herve, P.Y., Jobard, G., Petit, L., Crivello, F., Mellet, E., Zago, L., Mazoyer, B., Tzourio-Mazoyer, N., 2011. 'What is right-hemisphere contribution to phonological, lexico-semantic, and sentence processing? Insights from a meta-analysis. *Neuroimage* 54, 577–593. https://doi.org/10.1016/j.neuroimage.2010.07.036.
Wang, M., Arteaga, D., He, B.J., 2013. Brain mechanisms for simple perception and bistable perception. Proc. Natl. Acad. Sci. U.S.A. 110, E3350–E3359. https://doi.org/10.1073/pnas.1221945110.
Watanabe, T., Rees, G., 2017. Brain network dynamics in high-functioning individuals with autism. Nat. Commun. 8, 16048. https://doi.org/10.1038/ncomms16048.
Watanabe, T., Hirose, S., Wada, H., Imai, Y., Machida, T., Shirouzu, I., Konishi, S., Miyashita, Y., Masuda, N., 2013. A pairwise maximum entropy model accurately describes resting-state human brain networks. Nat. Commun. 4, 1370. https://doi.org/10.1038/ncomms2388.
Watanabe, T., Masuda, N., Megumi, F., Kanai, R., Rees, G., 2014. Energy landscape and dynamics of brain activity during human bistable perception. Nat. Commun. 5, 4765. https://doi.org/10.1038/ncomms5765.
Wilson, S.M., Schneck, S.M., 2021. Neuroplasticity in post-stroke aphasia: A systematic review and meta-analysis of functional imaging studies of reorganization of language processing. Neurobiol. Lang. (Camb) 2, 22–82. https://doi.org/10.1162/nol_a_00025.
Winhuisen, L., Thiel, A., Schumacher, B., Kessler, J., Rudolf, J., Haupt, W.F., Heiss, W.D., 2005. Role of the contralateral inferior frontal gyrus in recovery of language function in poststroke aphasia: a combined repetitive transcranial magnetic stimulation and

positron emission tomography study. Stroke 36, 1759–1763. https://doi.org/10.1161/01.STR.0000174487.81126.ef.
Winhuisen, L., Thiel, A., Schumacher, B., Kessler, J., Rudolf, J., Haupt, W.F., Heiss, W.D., 2007. The right inferior frontal gyrus and poststroke aphasia: a follow-up investigation. Stroke 38, 1286–1292. https://doi.org/10.1161/01.STR.0000259632.04324.6c.
Wolynes, P.G., 2015. Evolution, energy landscapes and the paradoxes of protein folding. Biochimie 119, 218–230. https://doi.org/10.1016/j.biochi.2014.12.007.
Xia, M., J. Wang, Y. He. 2013. BrainNet Viewer: a network visualization tool for human brain connectomics, *Plos One*, 8: e68910. https://doi.org/10.1371/journal.pone.0068910.
Xing, S., Lacey, E.H., Skipper-Kallal, L.M., Jiang, X., Harris-Love, M.L., Zeng, J., Turkeltaub, P.E., 2016. Right hemisphere grey matter structure and language outcomes in chronic left hemisphere stroke. Brain 139, 227–241. https://doi.org/10.1093/brain/awv323.
Xu, N., Doerschuk, P.C., Keilholz, S.D., Spreng, R.N., 2021. Spatiotemporal functional interactivity among large-scale brain networks. Neuroimage 227, 117628. https://doi.org/10.1016/j.neuroimage.2020.117628.
Xu, M., Liang, X., Ou, J., Li, H., Luo, Y.J., Tan, L.H., 2020. Sex Differences in Functional Brain Networks for Language. Cereb. Cortex 30, 1528–1537. https://doi.org/10.1093/cercor/bhz184.
Yang, X., Li, H., Lin, N., Zhang, X., Wang, Y., Zhang, Y., Zhang, Q., Zuo, X., Yang, Y., 2019. Uncovering cortical activations of discourse comprehension and their overlaps with common large-scale neural networks. Neuroimage 203, 116200. https://doi.org/10.1016/j.neuroimage.2019.116200.
Zhang, B., Wolynes, P.G., 2017. Genomic Energy Landscapes. Biophys. J. 112, 427–433. https://doi.org/10.1016/j.bpj.2016.08.046.
Zhu, Y., Bai, L., Liang, P., Kang, S., Gao, H., Yang, H., 2017. Disrupted brain connectivity networks in acute ischemic stroke patients. Brain Imaging Behav. 11, 444–453. https://doi.org/10.1007/s11682-016-9525-6.
Zhu, Y., Liu, J., Ye, C., Mathiak, K., Astikainen, P., Ristaniemi, T., Cong, F., 2020. Discovering dynamic task-modulated functional networks with specific spectral modes using MEG. Neuroimage 218, 116924. https://doi.org/10.1016/j.neuroimage.2020.116924.